HMG Advance Access published July 9, 2013

*Human Molecular Genetics, 2013* ***1–17***
*doi:10.1093/hmg/ddt302*

# Chemical genetics unveils a key role of mitochondrial dynamics, cytochrome *c* release and IP3R activity in muscular dystrophy

**Jean Giacomotto[1,2,3,*], Nicolas Brouilly[2,3], Ludivine Walter[2,3], Marie-Christine Mariol[2,3], Joachim Berger[4], Laurent Ségalat[2,3], Thomas S. Becker[1], Peter D. Currie[4] and Kathrin Gieseler[2,3,*]**

[1]Brain and Mind Research Institute, Sydney Medical School, University of Sydney, NSW 2050, Australia, [2]Centre de Génétique et de Physiologie Moléculaires et Cellulaires, CNRS UMR 5534, Campus de la Doua, 16 rue Dubois, 69622 Villeurbanne, France, [3]Université Claude Bernard Lyon 1, 43 boulevard du 11 Novembre, 69622 Villeurbanne, France and [4]Australian Regenerative Medicine Institute, Monash University, Clayton, VIC, Australia

Received May 1, 2013; Revised and Accepted June 21, 2013

**Duchenne muscular dystrophy (DMD) is a neuromuscular disease caused by mutations in the dystrophin gene. The subcellular mechanisms of DMD remain poorly understood and there is currently no curative treatment available. Using a *Caenorhabditis elegans* model for DMD as a pharmacologic and genetic tool, we found that cyclosporine A (CsA) reduces muscle degeneration at low dose and acts, at least in part, through a mitochondrial cyclophilin D, CYN-1. We thus hypothesized that CsA acts on mitochondrial permeability modulation through cyclophilin D inhibition. Mitochondrial patterns and dynamics were analyzed, which revealed dramatic mitochondrial fragmentation not only in dystrophic nematodes, but also in a zebrafish model for DMD. This abnormal mitochondrial fragmentation occurs before any obvious sign of degeneration can be detected. Moreover, we demonstrate that blocking/delaying mitochondrial fragmentation by knocking down the fission-promoting gene *drp-1* reduces muscle degeneration and improves locomotion abilities of dystrophic nematodes. Further experiments revealed that cytochrome *c* is involved in muscle degeneration in *C. elegans* and seems to act, at least in part, through an interaction with the inositol trisphosphate receptor calcium channel, ITR-1. Altogether, our findings reveal that mitochondria play a key role in the early process of muscle degeneration and may be a target of choice for the design of novel therapeutics for DMD. In addition, our results provide the first indication in the nematode that (i) mitochondrial permeability transition can occur and (ii) cytochrome *c* can act in cell death.**

## INTRODUCTION

Duchenne muscular dystrophy (DMD, OMIM 310200) is the most prevalent X-linked recessive neuromuscular disorder, affecting striated and cardiac muscles with an incidence of 1 out of 3000 male births. It is caused by mutations in the dystrophin gene (1). Dystrophin is a large cytoskeletal protein that links the cytoskeleton to the extracellular matrix (2).

Current treatments for DMD consist of long-term medication with the steroid prednisone, physiotherapy and specific bracing, but these interventions only slightly prolong ambulation in patients (3). Moreover, since severe side effects often accompany prednisone treatment, it is debatable whether its benefits outweigh its adverse effects. Therefore, the search for efficient palliative treatments is of great value. In addition, identifying the mechanism of action of beneficial drugs may help to understand better the physiopathology of this genetic disease.

The nematode *Caenorhabditis elegans* exhibits 95 striated body-wall muscle cells that are distributed in four longitudinal bands, named quadrants (Supplementary Material, Fig. S1). These muscle cells do not fuse, are not able to regenerate and, to our knowledge, do not undergo inflammatory processes after damage. We previously developed a *C. elegans* model for

*To whom correspondence should be addressed. Tel: +61 291144208, Fax: +61 293510599; Email: jean.giacomotto@sydney.edu.au, giacomottojean@gmail.com (J.G.); Tel: +33 472432951; Fax: +33 472432951; Email: kathrin.gieseler@univ-lyon1.fr (K.G.)

DMD (4). In this model, a mutation in the dystrophin gene, *dys-1*, is coupled with a hypomorphic mutation in the *C. elegans* MyoD gene, *hlh-1* (Supplementary Material, Table S1). Single *dys-1(cx18)* mutants present only weak muscle degeneration. In adult worms, up to two muscle cells are occasionally absent. However, combined with the hypomorphic *hlh-1(cc561)* allele, the *dys-1(cx18)* allele leads to progressive paralysis due to extensive muscle degeneration, which is time- and activity-dependent (Supplementary Material, Video S1) (4). The degenerative phenotype is generally observed after actin filament staining with phallodin–rhodamine and can be quantified by scoring muscle cells with disrupted or absent actin filaments (Supplementary Material, Fig. S1). The use of this nematode model as a tool for chemical screens provides an alternative to traditional screening systems and fills the gap in seeking drugs against DMD (5,6). Indeed, this approach led to the identification of drugs that have been further validated in the *mdx* mouse model for DMD (7,8).

In mammals, the subcellular mechanisms that lead to muscle degeneration are poorly understood. It is, however, commonly accepted that loss of dystrophin function induces intracellular $Ca^{2+}$ overload. In *C. elegans*, $Ca^{2+}$ transients have also been found to play a critical role in the degenerative process. Reducing the activity of the L-type voltage-gated EGL-19 or the Ryanodine Receptor UNC-68 calcium channels in the nematode DMD model diminishes muscle degeneration (9,10).

Mitochondria are dynamic organelles whose morphology and function are controlled by a balance between fission and fusion events (11). Under normal physiologic conditions, fusion predominates and the mitochondrial network presents mostly tubular morphology (12). However, under particular conditions such as high intracellular $Ca^{2+}$ concentration, oxidative stress, aging or activation of apoptotic and necrotic signals, the dynamic balance is shifted to fission, leading to mitochondrial network fragmentation (13). In such conditions, mitochondrial permeability transition (mPT) of mitochondrial membranes and the opening of large pores called mitochondrial permeability transition pores (mPTP) can occur and cause the cytosolic release of apoptotic factors (14). One of the released factors is cytochrome *c*, which is known in mammals to trigger apoptosis through its interaction with APAF-1 (15). When mPT is not reversed in a timely manner, cytosolic accumulation of these factors can lead to cell death. Several studies have shown that a mitochondrial matrix prolyl *cis–trans* isomerase, cyclophilin D, controls $Ca^{2+}$ and reactive oxygen species-dependent mPT (16). Targeting cyclophilin D with chemicals, such as the specific cyclophilin inhibitor Debio025, can reduce apoptotic signals release and cell death (17).

Cyclosporine A (CsA) is well known as an immunosuppressive drug, which is generally used after organ transplantation to prevent rejection. This compound has the ability to bind cytosolic cyclophilin A to form a complex that inhibits calcineurin, thus leading to lower T cell activity and immune response (18). CsA was suspected to be beneficial for DMD patients, as they present chronic muscle inflammation potentially due to calcium-dependent activation of calcineurin (19). In addition, CsA also exerts a calcineurin-independent effect on mPTP opening through cyclophilin D inhibition (20).

Using the *C. elegans* DMD model as a chemical screening tool, we found that CsA reduces dystrophin-dependent muscle degeneration at low dose but loses its positive effect at high dose. Our data further indicate that its beneficial effect involves a *C. elegans* mitochondrial cyclophilin D homolog, CYN-1, suggesting an implication of mPT in muscle degeneration in *C. elegans*. This finding also provides the first indication that mPT can occur in *C. elegans* (reviewed in 21). Furthermore, we show that mitochondrial dynamics is dramatically affected at the early stages of muscle degeneration not only in dystrophic nematodes but also in a zebrafish model for DMD. Moreover, we demonstrate that knockdown of the fission-promoting gene *drp-1* reduces both mitochondrial fragmentation and muscle degeneration in dystrophic nematodes. This observation suggests (i) that mitochondrial fragmentation observed in dystrophic muscles is due to increased mitochondrial fission, and (ii) that mitochondrial fission plays a key role in the early process of muscle degeneration. We further demonstrate a role for cytochrome *c* and the inositol trisphosphate receptor (IP3R) calcium channel, ITR-1, in both mitochondrial fission and muscle degeneration. Thus, our study also unveils for the first time, to our knowledge, that in *C. elegans* cytochrome *c* is involved in muscle cell death by acting, at least partially, through an interaction with IP3R/ITR-1.

## RESULTS

### CsA reduces muscle degeneration in dystrophin-deficient nematodes

Using the *C. elegans dys-1; hlh-1* model for DMD to search for potential bioactive drugs against muscle degeneration, we found that worms grown on agar medium supplemented with 100 nM CsA moved better than control animals treated with the solvent DMSO. Examination of body-wall muscle cells after phalloidin–rhodamine staining revealed a reduction of muscle degeneration by $>50\%$ (Fig. 1A and 2D; Supplementary Material, Fig. S1). Dose–response experiments showed an optimal effect of CsA against muscle degeneration at concentrations between 10 and 100 nM (Fig. 1A). This beneficial effect gradually decreased with lower doses, and was no longer significant at 0.1 nM and below. The beneficial effect of CsA on muscle degeneration of *dys-1; hlh-1* double mutants was lost at high dose. Above 10 μM, CsA exhibited no significant effects on muscle degeneration (Fig. 1A). At 100 μM, it induced moderate growth retardation, and at a concentration of $\geq 500$ μM it induced lethality (Fig. 1A).

Muscle degeneration in the worm model for DMD is caused by the synergistic effect of the *dys-1* and *hlh-1* mutations, as the mild *hlh-1(cc561)* mutation serves as an amplifier of the *dys-1(cx18)* phenotype. To confirm a specific effect on the *dys-1*-dependent phenotype, CsA was also tested at a concentration of 100 nM on *dys-1* single mutants and we found that it led to a significant decrease of muscle degeneration compared with control worms (Supplementary Material, Fig. S2A).

Muscle degeneration in the nematode is both activity- and time-dependent. Consequently, chemicals that have a sedative effect or that slow down development can reduce muscle degeneration. To exclude the possibility that CsA acted through these indirect effects, we analyzed its impact on mobility and growth rate. At a concentration of 100 nM in the medium, CsA had no significant impact on the growth rate of *dys-1; hlh-1* double

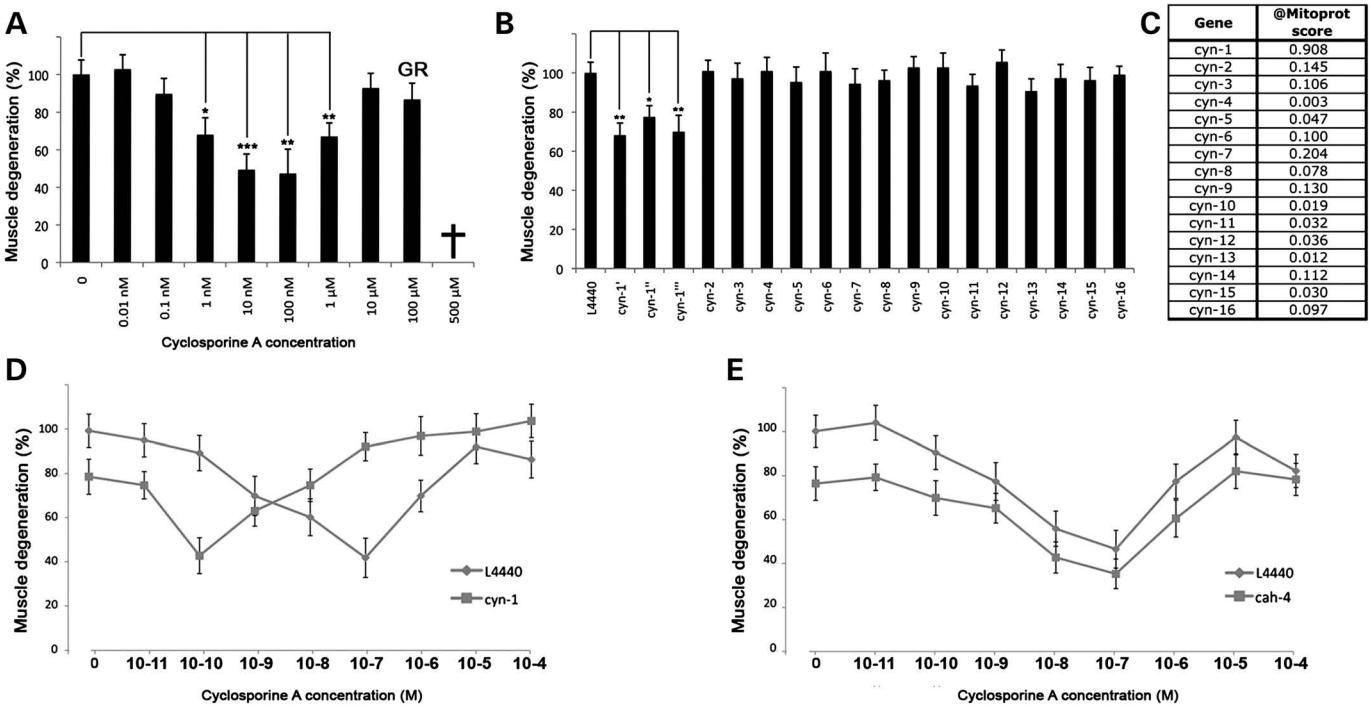


**Figure 1.** Pharmacologic and genetic inhibition of cyclophilin in LS587 *dys-1(cx18); hlh-1(cc561)* mutant animals. (**A**) Dose–effect of cyclosporine A (CsA) on muscle degeneration in the *C. elegans* DMD model LS587 *dys-1(cx18); hlh-1(cc561)*. (**B**) Effect of cyclophilin knockdown by RNAi on muscle degeneration in the *dys-1(cx18); hlh-1(cc561)* mutant animals. Nematodes were grown on bacteria producing dsRNA for *cyn-1* to *-16* or on bacteria carrying the empty L4440 plasmid (negative control). cyn-1′, cyn-1″, cyn-1‴ correspond to independent repeats of the same experiment. (**C**) Mitoprot value score for different *C. elegans* cyclophilin protein sequences. The Mitoprot software was used to predict the probability of mitochondria targeting of the 16 cyclophilin orthologs CYN-1 to -16. (**D**) Dose–response curve of CsA on muscle degeneration in the *dys-1(cx18); hlh-1(cc561)* mutant animals subjected to *cyn-1* RNAi or control RNAi (empty L4440 plasmid). (**E**) Dose–response curve of CsA on muscle degeneration in the *dys-1(cx18); hlh-1(cc561)* mutant animals subjected to *cah-4* RNAi (red curve) or control RNAi (empty L4440 plasmid, blue curve). Animals were grown for 8 days at 15°C. Means of 20 nematodes ± standard error of the mean. Different from control at $^{*}P < 0.05$, $^{**}P < 0.01$, $^{***}P < 0.001$. †Lethal; GR, growth retardation.

mutants, *dys-1* single mutants or wild-type worms (Supplementary Material, Fig. S2B). In addition, a concentration of 100 nM of CsA had no effect on the locomotion of *dys-1* single mutants or wild-type worms but significantly improved the mobility of *dys-1; hlh-1* double mutants (Supplementary Material, Fig. S2C). These results demonstrated that the beneficial effect of CsA on muscle degeneration in the *dys-1; hlh-1* double mutants was due to an improvement of muscle functions rather than to a sedative effect or reduced growth rate.

## Genetic inhibition of the mitochondrial cyclophilin D ortholog, CYN-1, mimics CsA treatment

In mammals, CsA has both an anti-inflammatory effect via calcineurin inhibition and an inhibitory effect on mPTP opening through cyclophilin D. As inflammatory responses are unlikely to contribute to muscle injuries in *C. elegans*, we tested whether the genetic inhibition of cyclophilin D could reduce muscle degeneration in *C. elegans*. Blast experiments using murine cyclophilin protein sequences (NP_032933.1, AAA37511.1, AAH19778.1, AAH45154.1, AAH04041.1, AAI50695.1) led to the identification of 16 cyclophilin orthologs in the nematode, named CYN-1 to -16. RNAi experiments were conducted in the DMD worm model to knockdown the expression of the corresponding genes. Only the RNAi-mediated knockdown of *cyn-1* led to a significant reduction of muscle degeneration (Figs 1B and 2D). Examination of the CYN-1 protein sequence revealed a close homology to cyclophilin D (Supplementary Material, Fig. S3). Moreover, the Mitoprot software revealed the presence of a 21-amino-acid mitochondrial targeting sequence required for mitochondrial translocation, and predicted a probability of mitochondrial export of >90% (22) (Fig. 1C). CYN-1 seems to be the sole mitochondrial cyclophilin in *C. elegans* as the Mitoprot score for the 15 other cyclophilin orthologs ranged from 0 to maximal 20% (Fig. 1C). Finally, as observed with CsA treatment, the RNAi-mediated knockdown of *cyn-1* did not modify the growth rate of *dys-1; hlh-1* double mutants, *dys-1* single mutants or wild-type worms (Supplementary Material, Fig. S2B). *cyn-1* RNAi further had no effect on the locomotion of *dys-1* single mutants or wild-type worms, whereas the mobility of *dys-1; hlh-1* double mutants was significantly improved (Supplementary Material, Fig. S2C).

## CsA acts through CYN-1 inhibition to reduce muscle degeneration

To determine whether the beneficial effects of CsA and *cyn-1* RNAi could be mediated through common mechanisms, muscle degeneration was quantified in *dys-1; hlh-1* double mutants treated with different doses of CsA and subjected or not to *cyn-1* RNAi (Fig. 1D and 2D). Worms subjected to

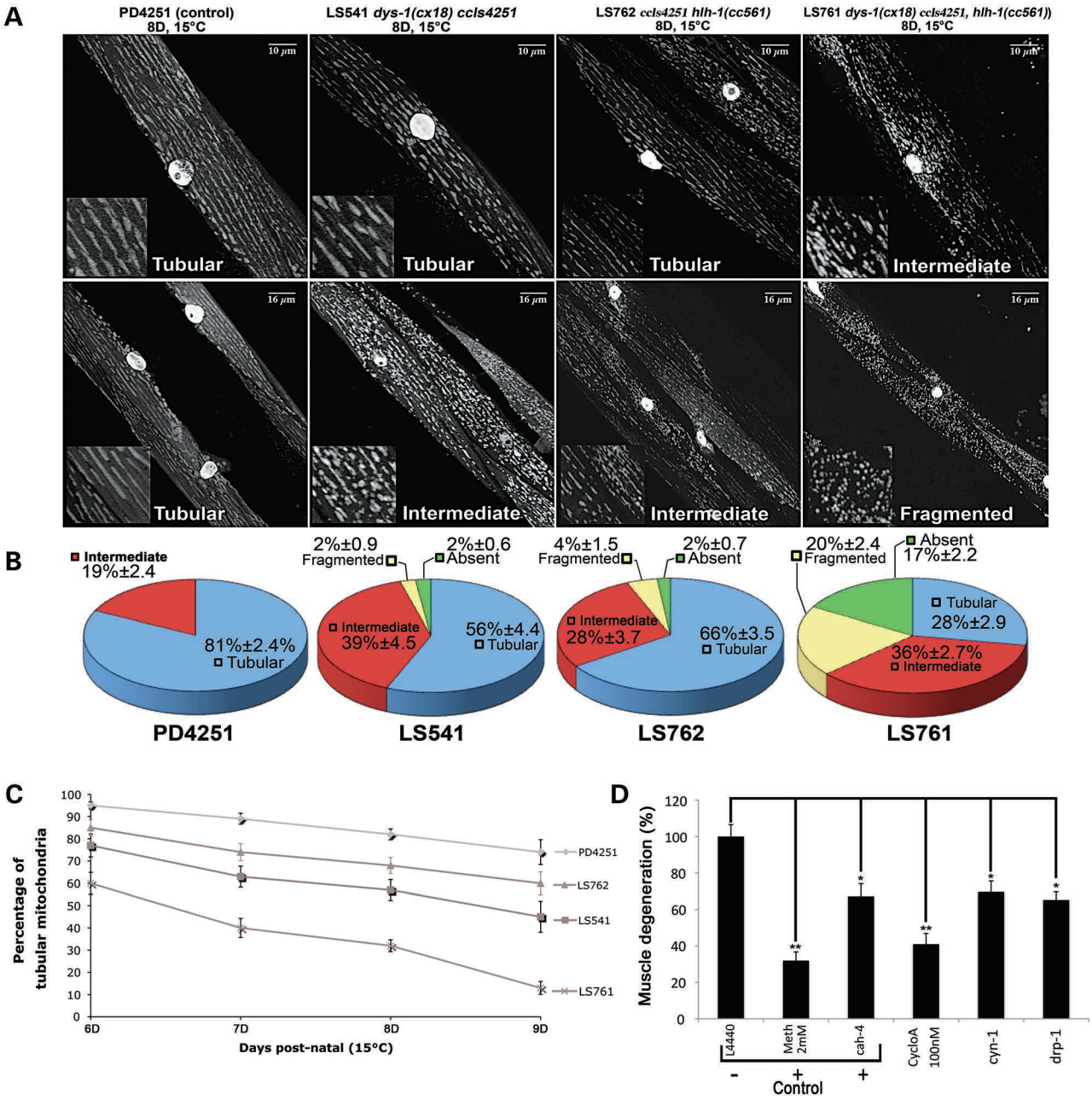


**Figure 2.** Mitochondrial network morphology and dynamics in muscle cells of *C. elegans*. (**A**) Representative images of the mitochondrial network organization visualized with GFP in muscle cells of transgenic *C. elegans* carrying the *ccIs4251* transgene in different genetic contexts. We evaluated mitochondrial network morphology by discriminating four types of mitochondria shapes: tubular, fragmented, intermediate or absent. (**B**) Mitochondrial morphology distribution per animal (one quadrant of all body-wall muscle cells has been observed per animal). For (A) and (B), animals were grown for 8 days (8D) at 15°C. (**C**) Mitochondrial dynamics observed in muscle cells of *C. elegans* over time. Animals were grown for 6 to 9 days at 15°C. (**D**) Effects of drug and RNAi-mediated knockdown treatment against muscle degeneration in the nematode DMD model LS587 *dys-1(cx18); hlh-1(cc561)*. Animals were grown for 8 days at 15°C. For RNAi-mediated knockdown experiments, nematodes were grown in the presence of DMSO on bacteria carrying the empty L4440 vector (negative control) or bacteria producing dsRNA for *cyn-1*, *drp-1* or positive control carbonic anhydrase 4 (*cah-4*) RNAi. Drug treatments were performed with Meth (carbonic anhydrase inhibitor, known to reduce muscle degeneration, used as a positive control) or CsA. (B–D) Mean of 20 nematodes ± standard error of the mean. Different from negative control at $^{*}P < 0.05$, $^{**}P < 0.005$.

*cyn-1* RNAi were significantly more sensitive to CsA in comparison with control worms fed with bacteria carrying the empty L4440 RNAi plasmid. The optimal dose for CsA was shifted from $10^{-7}$ M in control worms to $10^{-10}$ M in *cyn-1* RNAi-treated worms. Similarly, the lowest significantly effective concentration was shifted from $10^{-10}$ M in control worms to $10^{-11}$ M in *cyn-1* RNAi-treated worms, and the highest significant concentration was shifted from $10^{-5}$ to $10^{-7}$ M (Fig. 1D). Toxic doses leading to growth retardation (100 μM) and lethality (500 μM) were not modified by *cyn-1* RNAi treatment,

suggesting that the observed toxicity was not related to CYN-1 inhibition. In contrast, RNAi constructs targeting *cyn-2* to *-16* failed to modify the CsA dose–response curve on muscle degeneration (data not shown). In order to verify the specificity of *cyn-1* RNAi on the effect of CsA, we performed the same dose–response experiments by knocking down the *cah-4* gene (*cah-4*, carbonic anhydrase 4). *cah-4* encodes one of the six putative carbonic anhydrases of the worm, and has previously been found to reduce muscle degeneration in *C. elegans* when knocked down by RNAi (8). The RNAi-mediated knockdown of *cah-4* failed to modify the profile of the CsA dose–response curve (Fig. 1E). Altogether, these results indicate that CsA and *cyn-1* knockdown act through common mechanisms to reduce muscle degeneration.

The close homology of the *C. elegans* CYN-1 protein with mouse cyclophilin D along with its putative mitochondrial localization and its effect on the dose–response curve of CsA suggests that mPT occurs in *C. elegans*, and that the genetic or pharmacologic inhibition of CYN-1 protects from muscle degeneration by blocking or delaying mPTP opening.

### Dystrophin-deficient nematodes present abnormal mitochondrial network morphology

Considering that mPT may be involved in the process of muscle degeneration, mitochondrial morphology and dynamics were analyzed. For this purpose, we took advantage of the *ccIs4251* transgene, which drives the expression of the green fluorescent protein (GFP) in body-wall muscle cells where GFP localizes to nuclei and mitochondria (23). This transgene was genetically introduced into dystrophin-deficient *dys-1(cx18)* and *dys-1(cx18); hlh-1(cc561)* as well as into *hlh-1(cc561)* mutants (Supplementary Material, Video S1, Table S1). The morphology of the mitochondrial network reflected by the GFP signal observed by confocal microscopy unveiled dramatic mitochondrial fragmentation in all analyzed strains compared with control worms (PD4251 strain) (Fig. 2A–C; Supplementary Material, Fig. S4). Eight-day-old adult control worms presented 81 $\pm$ 2.4% of muscle cells with tubular mitochondria. In *hlh-1* or *dys-1* single mutants, this proportion was reduced to 66 $\pm$ 3.5 and 56 $\pm$ 4.4%, respectively, whereas *dys-1(cx18); hlh-1(cc561)* double mutants exhibited only 32 $\pm$ 2.9% of cells with tubular-shaped mitochondria (Fig. 2B). Interestingly, *dys-1; hlh-1* double mutants presented 16 $\pm$ 2.1% of degenerating muscles cells, and *dys-1* and *hlh-1* single mutants 2 $\pm$ 0.7 and 2 $\pm$ 0.8%, respectively. Thus, it appears that the severity of the changes in mitochondrial network morphology was correlated with the muscle degeneration phenotype. Importantly, mitochondrial network modifications precede sarcomeric defects as observed by disrupted actin filaments stained with phalloidin–rhodamine (Supplementary Material, Fig. S5). Altogether, our data suggest that morphologic defects of mitochondria may be an early process in dystrophin-dependent muscle degeneration.

Mitochondrial fragmentation further increased with age, regardless of the considered strains (Fig. 2C). This pattern is in accordance with previous studies, which link mitochondrial fragmentation to the aging process of muscle cells (24). However, fragmentation progression of the mitochondrial network in muscles of *dys-1; hlh-1* double mutants is dramatically increased over time, as after 9 days of culture at 15°C only 13 $\pm$ 2.9% of muscle cells still presented tubular mitochondria compared with 74 $\pm$ 5.5% in the PD4251 control strain (Fig. 2C).

### Reducing mitochondrial fission reduces muscle degeneration

Mitochondrial phenotypes observed in the *dys-1; hlh-1* double mutant suggest that mitochondrial defects are involved in the muscle degenerative process. RNAi-mediated knockdown of the fission-promoting dynamin-related *drp-1* gene was carried out to establish whether the loss of the tubular mitochondrial shape detected in muscle cells of dystrophic worms was due to increased mitochondrial fission. Knockdown of *drp-1* by RNAi in *dys-1; hlh-1* double mutants reduced muscle degeneration by almost 40% compared with control worms (Fig. 2D). Growth rate remained unchanged in wild-type control worms as well as in *dys-1(cx18)* single and *dys-1; hlh-1* double mutants (Supplementary Material, Fig. S2B). Locomotion was not modified in *dys-1* single mutants or wild-type worms, whereas *drp-1* knockdown significantly improved locomotion abilities of *dys-1; hlh-1* double mutants (Supplementary Material, Fig. S2C). Moreover, LS761 *dys-1(cx18) ccIs4251; hlh-1(cc561)* mutants subjected to *drp-1* RNAi presented fewer muscle cells with fragmented mitochondria compared with control worms (Fig. 3). These data confirm that mitochondrial fission is likely to contribute to muscle degeneration in dystrophic nematodes and that reducing fission delays muscle degeneration progression.

### Mitochondrial network abnormality is also an early event of muscle degeneration in a zebrafish DMD model

Mitochondria pattern and distribution were analyzed in a zebrafish DMD model, named $dmd^{pc2}$ (25). Homozygous $dmd^{pc2+/+}$ embryos and larvae present many hallmarks of human DMD patients, including muscle degeneration, fibrosis and inflammatory response. The first obvious sign of muscle degeneration in $dmd^{pc2+/+}$ embryos is the detachment of some muscle fibers from their myotendinous junction starting at 3 days post-fertilization (d.p.f.). To visualize the mitochondrial network and dynamics in muscle fibers of homozygous $dmd^{pc2+/+}$ animals, a plasmid that drives the expression of mitochondria-targeted GFP in striated muscle was injected into one-cell-stage embryos obtained from heterozygous $dmd^{pc2+/-}$ incrosses. Similar to dystrophic *C. elegans* muscles, myofibers of dystrophin-deficient $dmd^{pc2+/+}$ zebrafish embryos and larvae exhibited fragmented mitochondria (Fig. 4; Supplementary Material, Fig. S6 and S7). All dystrophic muscle fibers that have detached from the myotendinous junction, and appeared retracted, presented a mitochondrial network with a pronounced fragmented pattern, similar to the pattern observed in chemical-induced muscle cell death (26) (Supplementary Material, Fig. S6). At 3 d.p.f., GFP-positive muscle fibers that did not present any signs of degeneration, as indicated by tears or detachment from the myotendenous junction, already exhibited a fragmented mitochondrial network compared with tubular mitochondria observed in the control sibling embryos (Fig. 4).

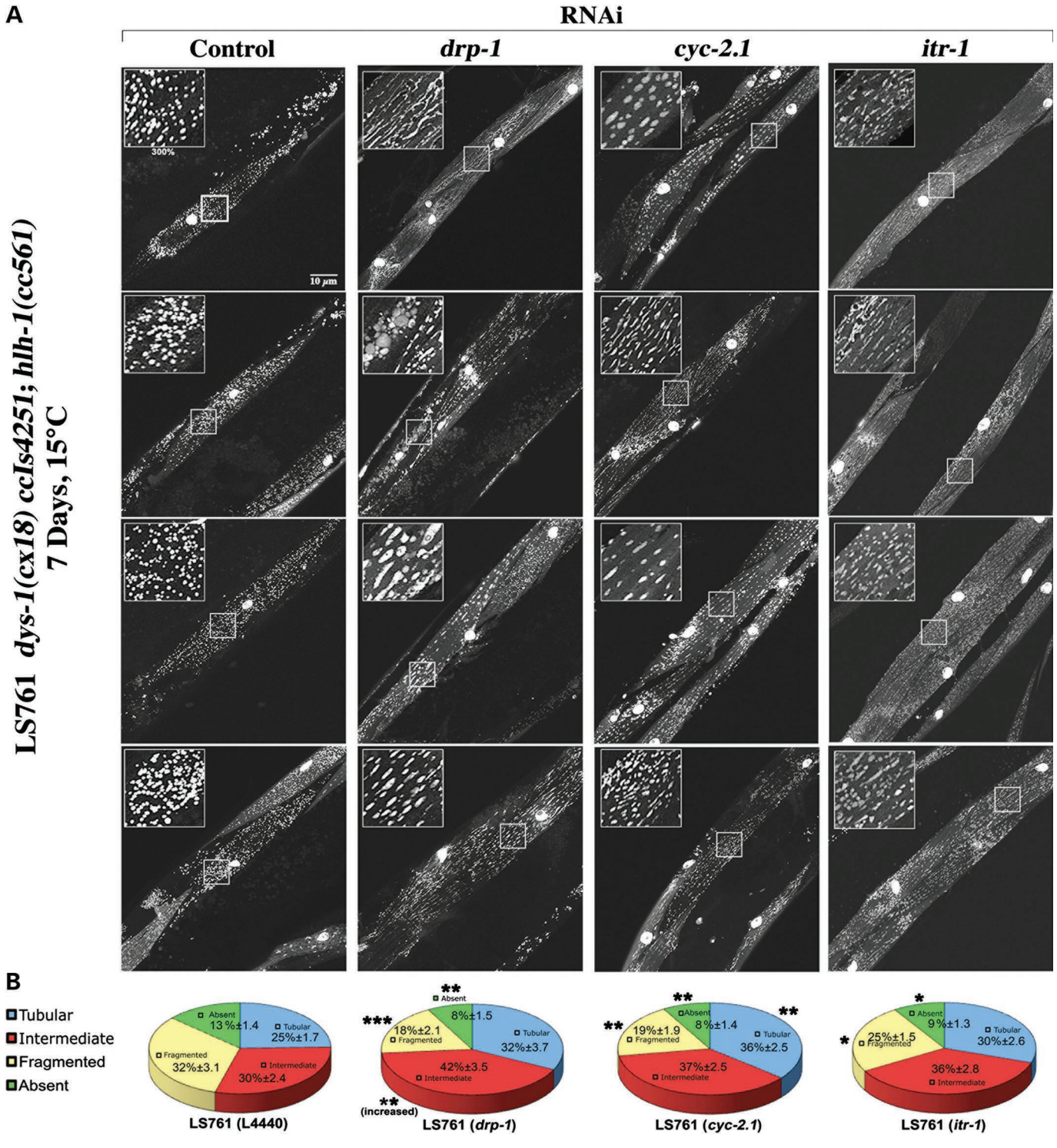


**Figure 3.** Effect of control, *drp-1*, *cyc-2.1* and *itr-1* RNAi on mitochondrial morphology of muscles in LS761 *dys-1(cx18) ccIs4251; hlh-1(cc561)* mutant nematodes. (**A**) Representative images of mitochondrial pattern observed in muscles of LS761 *dys-1(cx18) ccIs4251; hlh-1(cc561)* animals subjected to L4440 empty vector (control), *drp-1*, *cyc-2.1* or *itr-1* RNAi. (**B**) Distribution of muscle cells with fragmented, tubular, intermediate or absent mitochondrial network per animal. Animals were grown for 7 days at 15°C and were fed with dsRNA-expressing bacteria (*cyc-2.1* and *itr-1* RNAi treatment were starting from day 4). Mean of 20 nematodes ± standard error of the mean. Different from corresponding control L4440 at $^{*}P < 0.05$, $^{**}P < 0.02$, $^{***}P < 0.01$.

Moreover, at later stages (4 and 6 d.p.f.), GFP-positive fibers analyzed in homozygous *dmd*$^{pc2+/+}$ larvae, including those that were still attached to their corresponding myoseptum, exhibited a strongly fragmented mitochondrial pattern, whereas mitochondria of the control siblings were all tubular (Supplementary Material, Fig. S6 and S7). Altogether, these

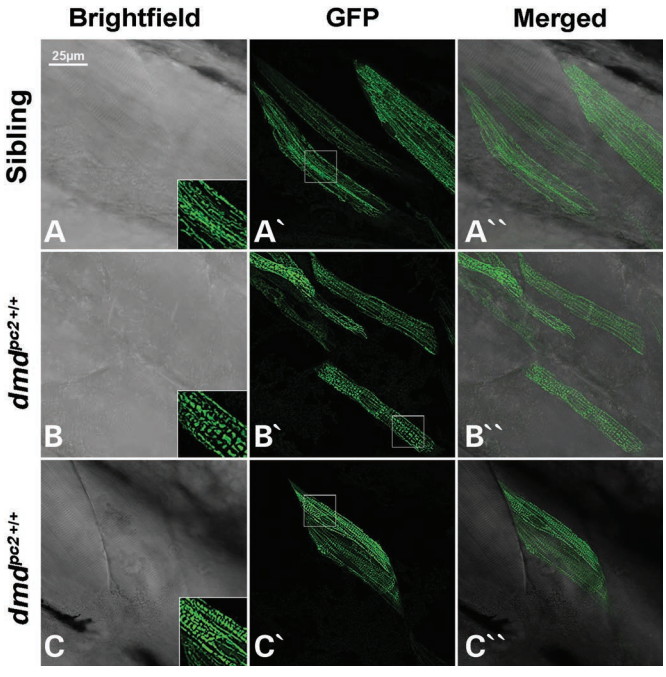


**Figure 4.** Representative images of the mitochondrial network observed in muscle fibers of 3 d.p.f. wild-type and *dmd*$^{pc2+/+}$ zebrafish embryos. (**A**) Tubular mitochondria of muscle fibers from control siblings. (**B** and **C**) Mitochondrial network in the *dmd*$^{pc2+/+}$ homozygote embryos. Mitochondria exhibit a fragmented pattern even in muscles without any other signs of muscle degeneration. At this stage, some muscle fibers presenting a highly fragmented mitochondrial network can be spotted in the *dmd*$^{pc2+/+}$ homozygote embryos; however, these fibers usually also present signs of tears at the myotendinous junction, suggesting an advanced stage of degeneration (see Supplementary Material, Fig. S7).

observations indicate that mitochondrial network alterations are early events in the process of dystrophin-dependent muscle degeneration in both *C. elegans* and zebrafish models for DMD.

### Cytochrome *c* is involved in *C. elegans* dystrophic muscle cell death

Inhibition of mitochondrial fission or cyclophilin D reduced muscle degeneration in dystrophic worms. We thus wondered whether interfering with pro-apoptotic factors released from mitochondria when mPT occurs would reproduce the effect of CsA treatment or of *cyn-1* RNAi on muscle degeneration. We focused on cytochrome *c*, which is well known to participate in cell death in mammals after being released from mitochondria (15,27). Based on the *C. elegans* database (www.wormbase.com) and on the murine sequence of cytochrome *c* (CAA25899.1), three genes were selected for further analysis: *cyc-1*, *cyc-2.1* and *cyc-2.2* (Supplementary Material, Table S2) (28). Only the knockdown of *cyc-2.1* significantly reduced muscle degeneration in *dys-1; hlh-1* double mutants (Fig. 5A). Knockdown of *cyc-1* led to lethality, whereas RNAi against *cyc-2.2* did not induce any detectable phenotype. However, *cyc-2.1* RNAi induced growth retardation when worms were treated starting from the first larval stage, thus hampering the readout of the time-dependent muscle degeneration phenotype (Fig. 5A and E). In order to ensure that the beneficial effect on muscle degeneration was not due to growth rate retardation, *cyc-2.1* RNAi treatment was started at different time points of the development of the worms. Muscle degeneration is usually scored in adult worms at day 8 of culture. Therefore, worms were cultured on bacteria unable to produce *cyc-2.1* dsRNA and transferred on *cyc-2.1* dsRNA-producing bacteria at different days of culture (days 2 to 7). When *cyc-2.1* RNAi treatment was initiated at day 3, 4 or 5 of worm culture, no growth retardation was detected and muscle degeneration was still significantly reduced (Fig. 5A and E). This genetic treatment significantly reduced the paralysis observed in *dys-1; hlh-1* double mutants, whereas it had no specific effect on locomotion behavior of *dys-1* single mutants or wild-type worms (Fig. 5F). *cyc-2.1* RNAi treatment started at day 6 or 7 had no detectable effect on muscle degeneration (Fig. 5A).

The tissue expression of *cyc-2.1* was then investigated through the expression of GFP driven by the putative promoter of *cyc-2.1*. At all larval stages as well as in adults, GFP expression was observed in the excretory cell, in the nervous system, in intestine cells, in the pharynx and in body-wall muscles (Fig. 6). In a majority of transgenic worms, a predominant expression was observed in the intestine and in muscle cells compared with other tissues expressing GFP. The strong expression in body-wall muscles is consistent with the observed effect of *cyc-2.1* RNAi-mediated knockdown on muscle degeneration.

### Cytochrome *c*/IP3R interaction is implicated in muscle degeneration

Finding cytochrome *c* to be involved in dystrophin-dependent muscle degeneration tends to confirm that mitochondria play a significant role in DMD. However, the *C. elegans* ortholog of APAF-1 encoded by the *ced-4* gene does not contain the WD40 repeat domain responsible for cytochrome *c* binding (29). It has, therefore, been assumed that, in *C. elegans*, cytochrome *c* is not involved in cell death. Our results thus provide the first evidence that cytochrome *c* can contribute to cell death in *C. elegans*. We then aimed to establish how cytochrome *c* contributes to muscle degeneration in dystrophic worms. In rats, cytochrome *c* was shown to bind to the cytosolic C-terminal sequence of type 1 IP3R (30). We, therefore, analyzed whether CYC-2.1 is able to bind to the *C. elegans* IP3R ortholog, ITR-1, and whether this interaction is involved in the muscle degenerative process in *dys-1; hlh-1* double mutants.

In mammals, the critical region responsible for the binding of cytochrome *c* has been attributed to the amino acids 2621–2636 of IP3R (31). This sequence is well conserved from invertebrates to humans (Fig. 7A and B). To ensure proper cloning of the putative cytochrome *c*-binding sequence—named in the following 'Sp-cyc', for cytochrome *c* sponge—a cDNA fragment carrying ITR-1 C-terminus encoding sequence starting from the end of the last transmembrane domain of ITR-1 and a second fragment encoding the same peptide fused to an HA-tag, Sp-cyc-HA, were generated (Fig. 7A).

The Sp-cyc- and Sp-cyc-HA-encoding fragments as well as a cDNA encoding the full-length CYC-2.1 protein were cloned into yeast two-hybrid bait and prey plasmids. Yeast two-hybrid experiments confirmed the interaction of both peptides, Sp-cyc and Sp-cyc-HA, with the full-length CYC-2.1 protein (Fig. 7C). In addition, Sp-cyc and Sp-cyc-HA peptides were able to interact with themselves, which is in accordance with a previous study that identified an oligomerization-binding site in the IP3R C-terminus (32).

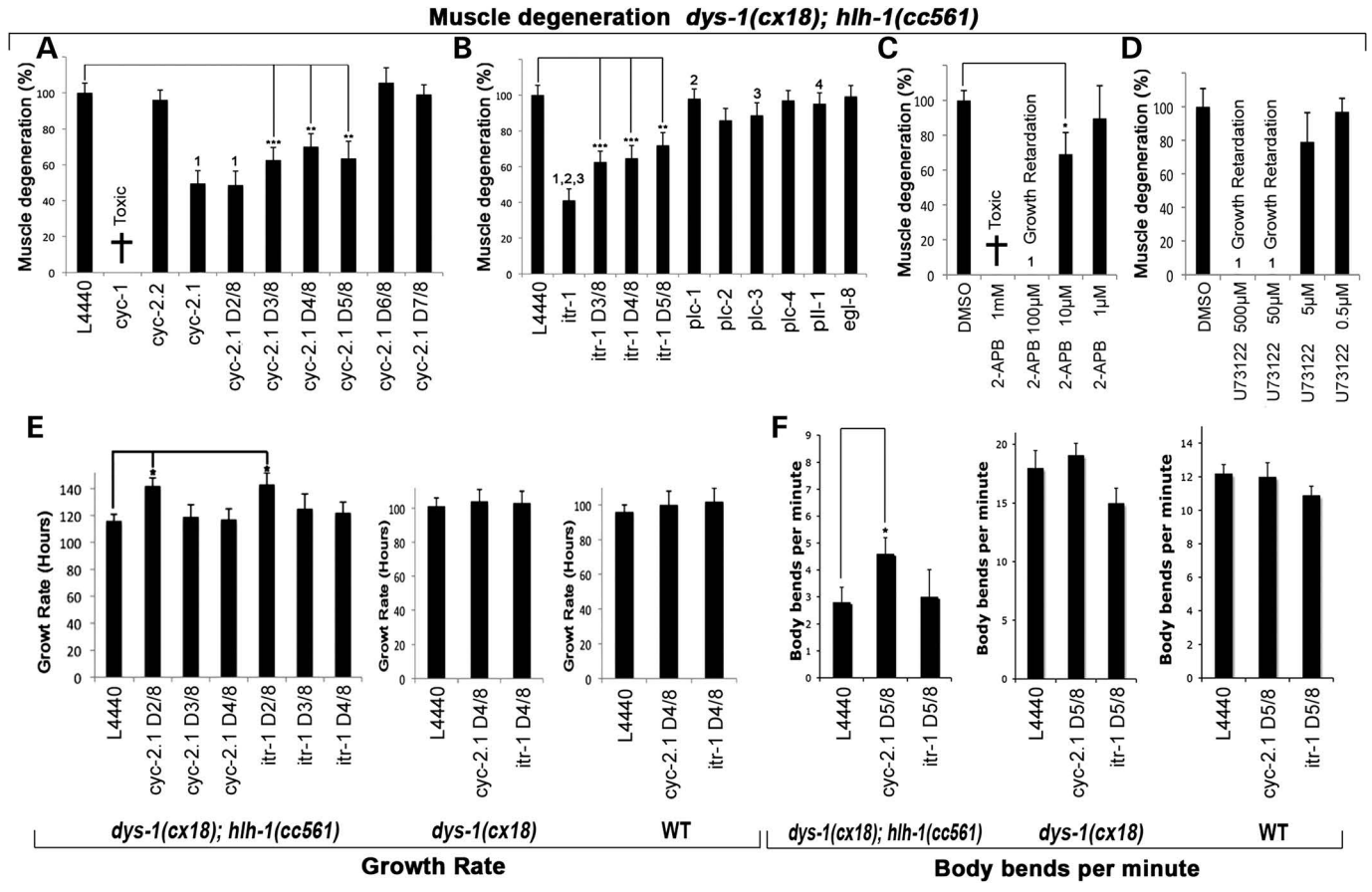


**Figure 5.** Effects of gene knockdowns and pharmacologic treatments on muscle degeneration, locomotion behavior and growth rate of nematodes. (**A**) Effects of RNAi-mediated knockdown of putative cytochrome *c* genes (*cyc-1, cyc-2.1* and *cyc-2.2*) on muscle degeneration in *dys-1(cx18); hlh-1(cc561)* mutant nematodes. (**B**) Muscle degeneration in *dys-1(cx18); hlh-1(cc561)* mutant nematodes after knockdown of the *C. elegans itr-1* gene, which encodes an ortholog of the mammalian IP3R family and of different genes (*plc-1* to *plc-4, pll-1* and *egl-18*) encoding putative orthologs of the main IP3R regulators, i.e. PLC. (**C** and **D**) Muscle degeneration in *dys-1(cx18); hlh-1(cc561)* animals after 2-APB or U-73122 exposure, respectively. (**E**) Effect of dsRNA exposure on growth rate of *dys-1(cx18); hlh-1(cc561)* double mutants, *dys-1(cx18)* single mutants, and wild-type (wt) worms. Growth rate corresponds to the time (in hours) from eggs to reproductive adult worms. (**F**) Effect of knockdown experiments on locomotion rate of *dys-1(cx18); hlh-1(cc561), dys-1(cx18)* and wild-type (wt) animals. Animals were grown for 8 days at 15°C. DX/8 correspond to days when animals were transferred from control plates (bacteria carrying the empty vector L4440) to plates seeded with bacteria expressing dsRNA (RNAi-mediated knockdown). Mean of 20 nematodes ± standard error of the mean. Different from control at $^{*}P < 0.05$, $^{**}P < 0.02$, $^{***}P < 0.01$. 1, growth retardation; 2, embryonic lethality; 3, sterility; 4, egg laying increased.

Subsequently, the Sp-cyc- and Sp-cyc-HA-encoding DNA fragments were expressed in *dys-1; hlh-1* double mutants under the control of the muscle promoter P*myo-3*. The HA-tagged peptides, Sp-cyc-HA, were detected in muscle cells by immunostaining, thus indicating that the constructs were correctly expressed (Fig. 7D).

Two independent lines per construct (expressing the Sp-cyc or Sp-cyc-HA peptide) were generated. In all these lines, a significant reduction of muscle degeneration was observed in transgenic worms compared with non-transgenic siblings (Fig. 7E). Moreover, owing to mosaic expression of transgenes in *C. elegans*, the peptides were expressed in only 50–70% of muscle cells, suggesting that their effects on muscle degeneration were under-evaluated in this study (Fig. 7D and 8).

Although the Sp-cyc and Sp-cyc-HA peptides are expressed during all developmental stages, no *itr-1* knockdown-like phenotypes such as growth retardation, sterility and embryonic lethality were observed in the transgenic lines (data not shown) (33). Moreover, the P*myo-3* promoter induced expression of the SP-cyc and Sp-cyc-HA peptides in body-wall muscle cells as well as in somatic contractile sheath cells. A previous study showed that the alteration of ITR-1 function in these cells leads to an inhibition of sheath contractile activity (34). In our experiments, sheath contraction cycles remained unchanged in the presence of the peptides, suggesting that the SP-cyc and Sp-cyc-HA peptides did not interfere with ITR-1 oligomerization and did not disturb endogenous ITR-1 function (data not shown).

These results suggest that, in *C. elegans*, cytochrome *c* can bind to ITR-1 and thereby contribute to muscle degeneration. Therefore, it is likely that the sponge peptides reduce muscle degeneration in the dystrophic worms by disturbing the interaction between cytochrome *c* and ITR-1.

## ITR-1 is required for muscle degeneration

The results obtained with cytochrome *c* sponges suggest that the calcium channel ITR-1 plays a role in dystrophin-dependent muscle degeneration. We, thus, analyzed the effect of *itr-1*

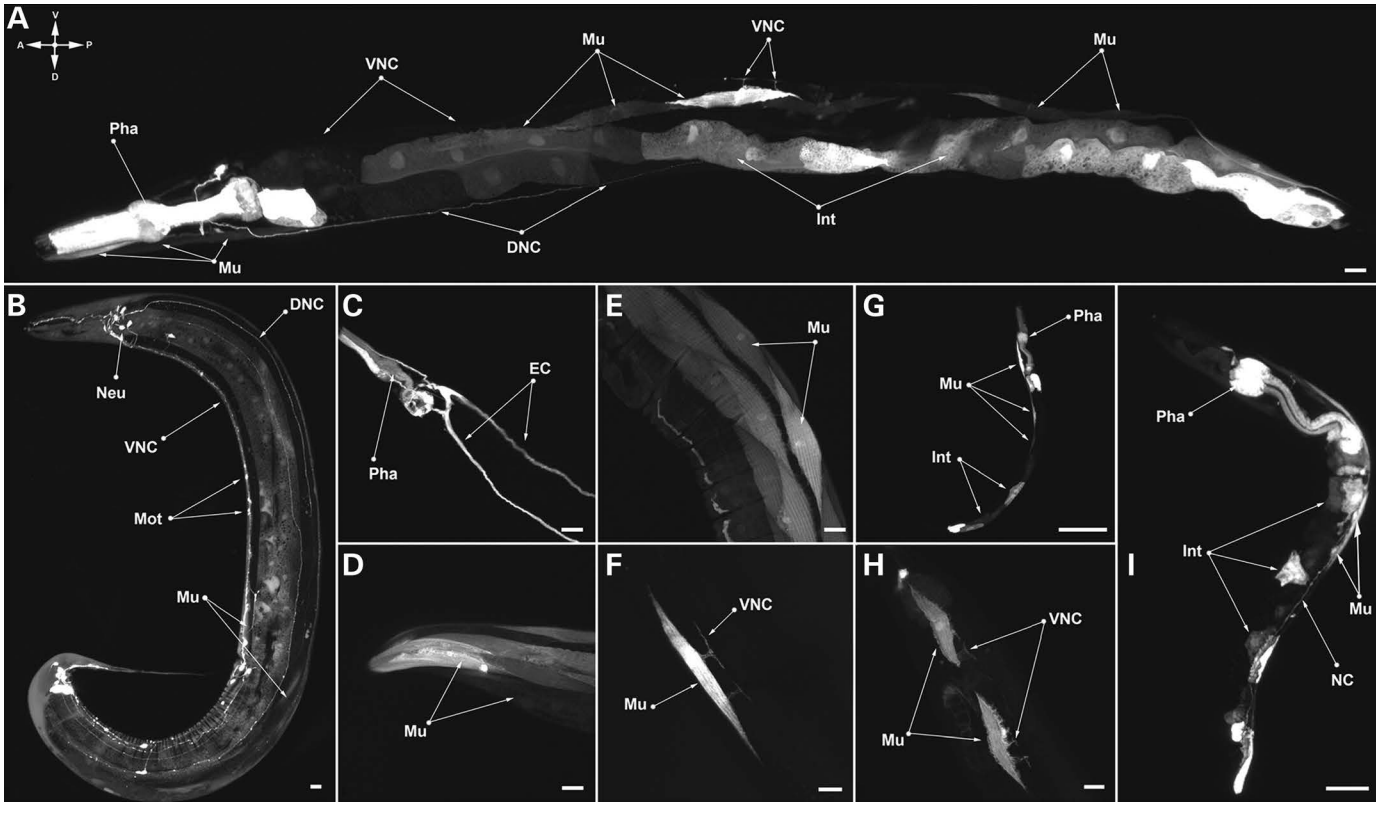


**Figure 6.** Tissue expression of *cyc-2.1* in *C. elegans*. The expression pattern of *cyc-2.1* was detected by the GFP reporter protein expressed under the control of the *cyc-2.1* promoter. Pha, pharynx; Mu, muscle cell; VNC, ventral nerve cord; DNC, dorsal nerve cord; Mot, motorneurone; EC, excretory cell; Int, intestine. Scale bar indicates 10 μm.

knockdown on muscle degeneration in *dys-1; hlh-1* double mutants. RNAi treatment against *itr-1* significantly reduced the number of degenerating muscle cells (Fig. 5B). According to previous studies, RNAi-mediated knockdown of *itr-1* induced growth retardation as well as sterility and embryonic lethality in the progeny of worms treated during the entire culture period of 8 days (Fig. 5B and E) (33). Therefore, dystrophic worms were subjected to *itr-1* RNAi at different time points of development. The aforementioned phenotypes were no longer detectable when worms were treated starting from day 3, whereas a significant beneficial effect on muscle degeneration was observed for all treatments starting from day 3, 4 or 5 of culture (Fig. 5B and E). In addition, this treatment did not affect locomotion or growth rate of *dys-1* single mutants and wild-type worms (Fig. 5E and F). However, the impact of *itr-1* knockdown on muscle degeneration was not accompanied by a significant gain of motility of *dys-1; hlh-1* double mutants (Fig. 5F). Finally, *dys-1; hlh-1* double mutants treated with the IP3R inhibitor aminoethoxydiphenyl borate (2-APB) showed significantly less muscle degeneration compared with control worms (Fig. 5C). These observations, thus, demonstrated a role for the ITR-1 calcium channel in muscle degeneration.

Since IP3R activity is mostly regulated by inositol trisphosphate (IP3), which is generated by phospholipase C (PLC), we further analyzed whether knocking down *C. elegans* PLC orthologs would reproduce the effects of *itr-1* RNAi. Six PLC orthologs encoding genes are known in *C. elegans*, named *plc-1* to *-4*, *pll-1* and *egl-8* (35) (Supplementary Material, Table S2). RNAi knockdown experiments against these genes did not lead to a significant reduction of muscle degeneration of *dys-1; hlh-1* double mutants (Fig. 5B). Combinatory experiments were also conducted but did not lead to significant outcomes (data not shown). In addition, the PLC inhibitor U-73122 failed to significantly modify muscle degeneration in *dys-1; hlh-1* double mutants (Fig. 5D).

## ITR-1 and cytochrome *c* play a role in both muscle degeneration and mitochondrial dynamics

Our results indicate that the interaction between ITR-1 and CYC-2.1 plays a role in muscle degeneration of dystrophic nematodes. We, thus, questioned whether these two proteins contribute to the fragmentation of the mitochondrial network observed in LS761 *dys-1(cx18) ccIs4251; hlh-1(cc561)* nematodes. LS761 animals subjected to *cyc-2.1* or *itr-1* RNAi-mediated knockdown starting from day 4 of culture presented not only significantly fewer degenerating muscle cells but also significantly less muscle cells with a fragmented mitochondrial pattern, compared with control worms (Fig. 3; Supplementary Material, Fig. S8). In addition, the expression of the sponge peptide Sp-cyc in the body-wall muscle cells of LS761 worms also led to a significant reduction of mitochondrial fragmentation in mCherry-positive muscle cells that inherited the construct compared with neighboring non-transgenic cells (Fig. 8).

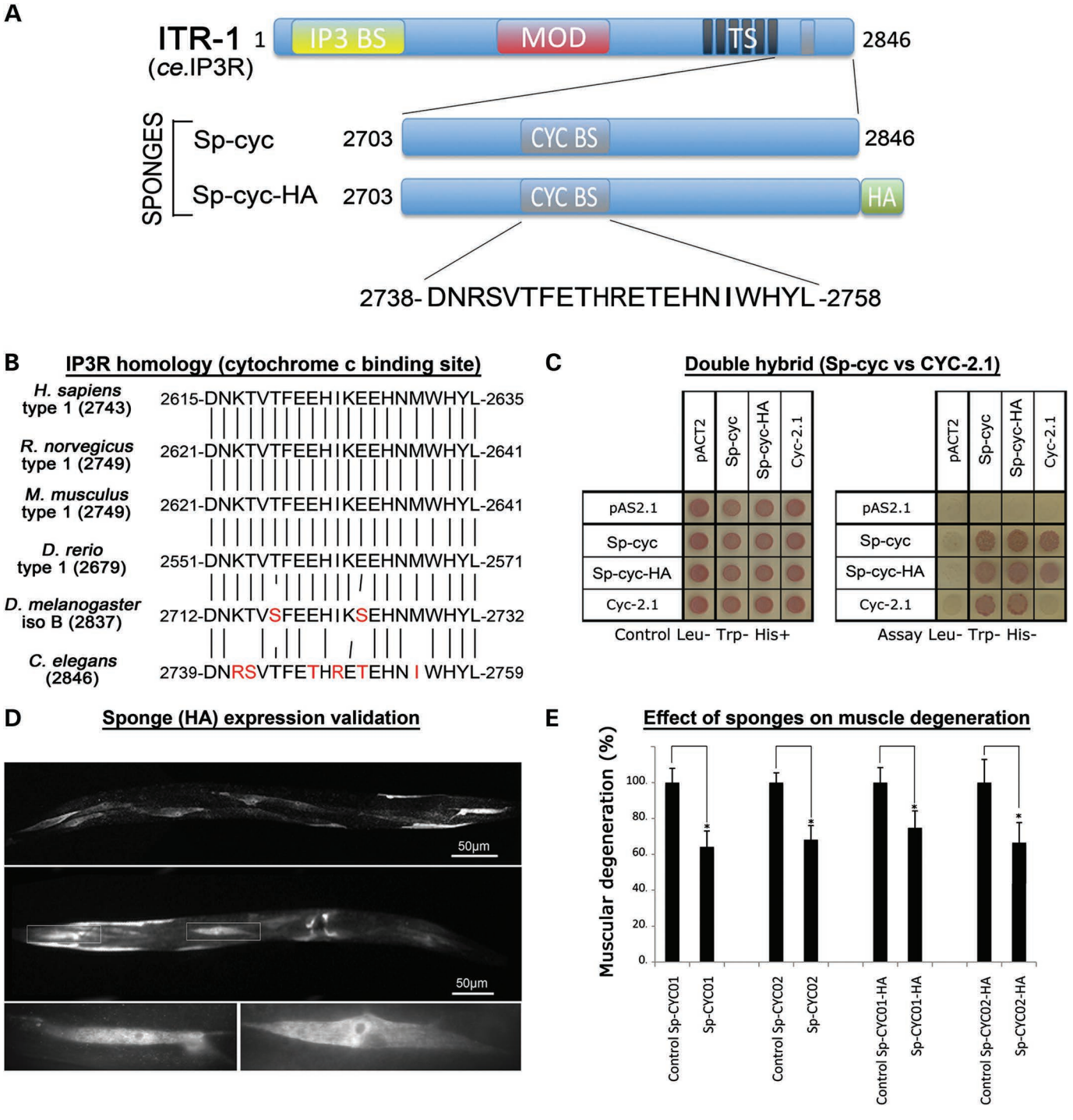


**Figure 7.** A peptide carrying the cytochrome *c*-binding sequence of *Ce*IP3R (ITR-1) reduces muscle degeneration. (**A**) Schematic representation of IP3R protein (named ITR-1 in *C. elegans*), and the ITR-1 sequence used to construct cytochrome *c* sponges, with or without an N-terminal HA-tag (SP-cyc-HA and SP-cyc, respectively). IP3BS, IP3-binding site; MOD, modulatory domain; TS, transmembrane domain; CycBS, cytochrome *c*-binding site; HA, tag HA. (**B**) Comparison of cytochrome *c*-binding sequence of IP3R proteins among different species. (**C**) Two-hybrid experiments conducted to validate the putative interaction between CYC-2.1 and the ITR-1 calcium channel. Left panel: growth control for diploid yeasts carrying both a bait and a prey plasmid on culture medium lacking leucine and tryptophan and supplemented with histidine; right panel: diploid yeasts carrying both a bait and a prey plasmid on culture medium lacking leucine, tryptophan and histidine; diploid yeasts can grow only if the prey (columns) and bait (lines) proteins interact. Empty pAS2.1 bait and pACT2 prey plasmids were used for negative controls. (**D**) Muscular expression validation of the HA-tagged cytochrome *c* sponge construct, SP-cyc-HA in N2 worms. Mosaic expression was detected in body-wall muscle cells as well as in vulva muscle cells. (**E**) Effect of the different cytochrome *c* sponges, SP-cyc-HA and SP-cyc upon muscle degeneration in the LS761 *dys-1(cx18) ccIs4251; hlh-1(cc561)* strain. Animals were grown for 8 days at 15°C. Mean of 20 worms ± standard error of the mean.

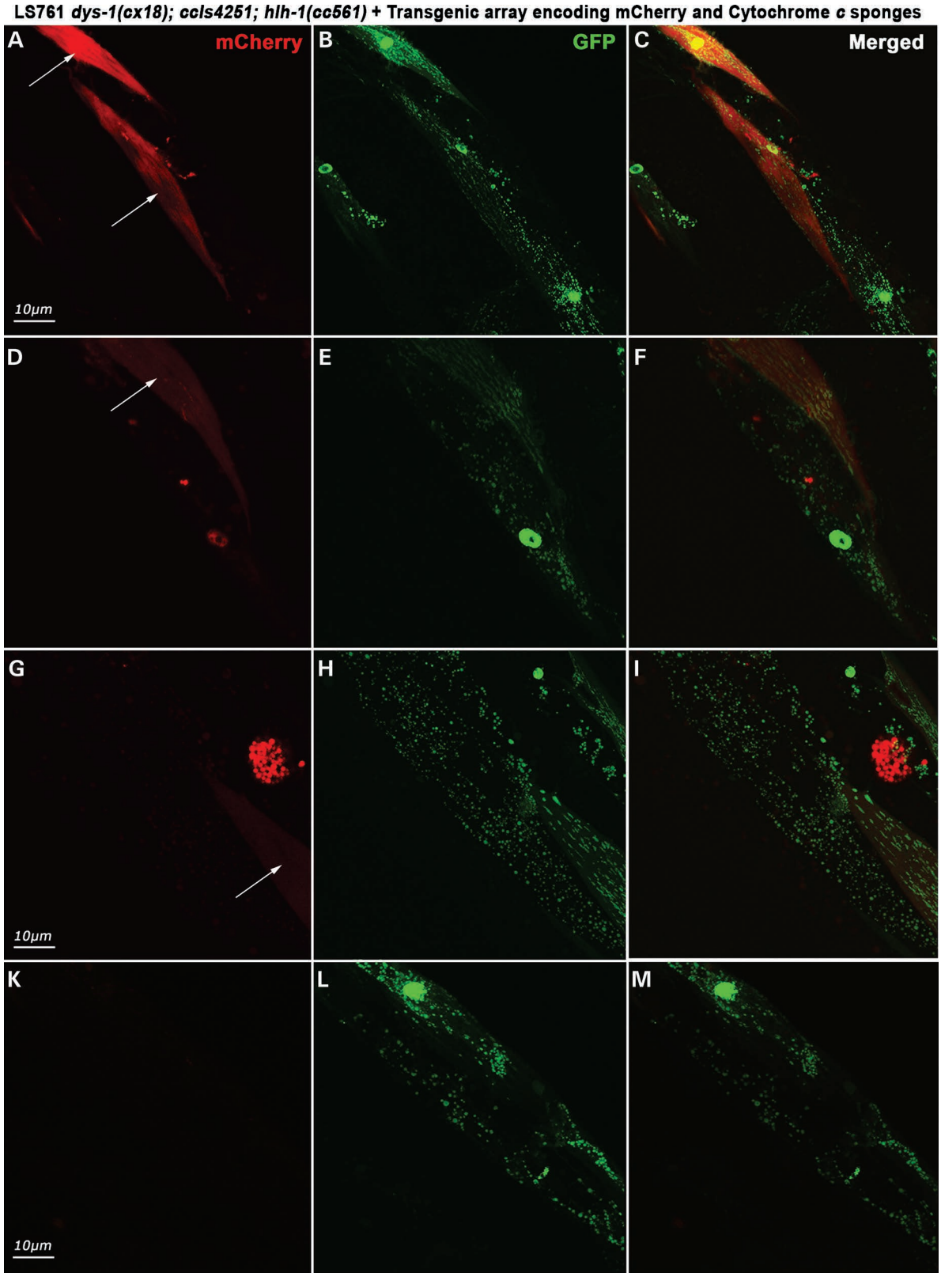


**Figure 8.** Cytochrome *c* sponge expression and mitochondria morphology in LS761 *dys-1(cx18); ccIs4251; hlh-1(cc561)* nematodes. Cells expressing the transgenic array encoding mCherry and the ITR-1 C-terminus (SP-cyc) are pointed by white arrows and present tubular mitochondrial network compared with non-transgenic neighboring muscle cells, which exhibit mostly fragmented mitochondria. Animals were grown for 8 days at 15°C.

These results suggest that ITR-1 and CYC-2.1 and their interaction contribute to both altered mitochondrial dynamics and muscle degeneration observed in dystrophic nematodes.

## DISCUSSION

Here, we demonstrate that CsA is beneficial toward dystrophin-dependent muscle degeneration in the nematode *C. elegans*. Efficient doses of CsA upon muscle degeneration range from 1 nM to 1 μM in the culture medium, thus revealing a high efficiency and bioavailability of the drug into the nematode. Indeed, most of the drugs identified as being beneficial toward muscle degeneration in the nematode DMD model presented an optimal effect in a dose range from 100 μM to 2 mM in the medium [(8), L.S., unpublished results]. Similar results have been reported within the *mdx* mouse model. Administration of 10 mg/kg/day of CsA by feeding led to improvement of outcomes in *mdx* mice and suggested that this compound may be of interest for humans (19). However, a recent clinical trial showed that this drug, when delivered at relative high dose (4 mg/kg/day), did not significantly improve muscle functions of DMD patients (36). Our results show that, in the *C. elegans* DMD model, CsA treatment loses its beneficial effect against muscle degeneration when used at doses $>10$ μM in the medium. Accordingly, high-dose treatment of *mdx* mice (30 mg/kg/day intraperitoneally) did not lead to any benefit, and was rather deleterious for muscles in the dystrophic context (37). Considering body surface area normalization method, administration to a child of 4 mg/kg/day of a drug corresponds to ∼33 mg/kg/day in adult mice (38). This dose might thus be too high to induce any beneficial effect in humans. It is noteworthy that no deleterious effect of the drug was reported in the human trial. The deleterious effect in mice was attributed to an interference with muscle regeneration due to calcineurin inhibition. Besides lethal toxicity at the highest dose tested, no deleterious muscular effect was observed in *C. elegans*, which is potentially due to the lack of muscle regenerative processes in the nematode. It is also well established that mice possess a more effective regenerative capacity than humans, which may also explain that no deleterious effect on muscles was reported in the human trial. So far, results obtained with *C. elegans* and mice suggest that the optimal dose of CsA that could lead to potential beneficial effects may have been missed in humans.

CsA was initially suspected to be beneficial against the inflammatory processes that take place in the muscles of DMD patients and *mdx* mice (19,36). However, since *C. elegans* lacks an inflammatory system, at least in muscles, finding CsA to be beneficial toward dystrophin-dependent muscle degeneration supports the hypothesis that the effect of this compound on muscle degeneration involves mechanisms other than immunosuppression. Our study shows that, in the nematode, low doses of CsA act, at least in part, through cyclophilin D to reduce muscle degeneration. Interestingly, the CsA analog Debio025 was also found to improve the outcomes in *mdx* mice (39). Since Debio025 lacks immunosuppressive activity, it has been suggested that this drug reduces muscle degeneration through the regulation of mPTP opening. This hypothesis was further supported by the observation that genetic inhibition of cyclophilin D improves *mdx* mouse phenotypes, reinforcing the relevance of this protein as a potential therapeutic target against DMD (40). In addition, cyclophilin D was further linked to muscle cell death in collagen VI myopathic mice, thus suggesting that cyclophilin D inhibition may be relevant as a treatment for myopathies in general (41).

The relevance of cyclophilin D as a therapeutic target is also confirmed by our observation of a key role for mitochondrial dynamics in the early process of muscle degeneration in *C. elegans* and most likely in zebrafish. Cyclophilin D directly regulates calcium-dependent mPT and cellular necrosis. Mice lacking cyclophilin D present protection against necrotic cell death after ischemic injury, and mitochondria isolated from these mice are resistant to calcium-induced swelling (16). Cytosolic calcium overload has been observed in *mdx* mouse muscle fibers as well as in humans, and we previously showed that $Ca^{2+}$ transients play a critical role in the DMD nematode model (9). This excess of calcium may be up-taken by mitochondria, and thus lead to mPT, increased mitochondrial fission, as well as cytochrome *c* release, and all these phenomena may promote muscle cell degeneration. This hypothesis is further supported by our observations showing that inhibiting mPTP opening with CsA treatment and/or *cyn-1* knockdown, reducing mitochondrial fission with *drp-1* knockdown as well as inhibiting cytochrome *c* via *cyc-2.1* knockdown, all improve the dystrophic muscle phenotype in the *C. elegans* DMD model (Fig. 9).

The beneficial effect of cytochrome *c* knockdown toward dystrophic muscle tends to confirm that mitochondria play a significant role in dystrophin-dependent muscle degeneration. However, cytochrome *c* may not promote directly apoptosome formation in the nematode, as the *C. elegans* APAF-1 heterologous CED-4 lacks the cytochrome *c*-binding domain (29). Thus, in *C. elegans*, cytochrome *c* may promote muscle degeneration by contributing to the increase of $Ca^{2+}$ intake and accumulation in mitochondria through its interaction with the calcium channel IP3R, thereby amplifying subsequent events involved in cell death. Rizzuto *et al.* (42) demonstrated that IP3R is directly juxtaposed to mitochondria, and mediates $Ca^{2+}$ transient between these organelles. It has been further determined that cytochrome *c* interaction with the C-terminus of the IP3R is critical for $Ca^{2+}$ signaling in cell death, resulting in $Ca^{2+}$ poisoning of the mitochondria (31). The mitochondrial $Ca^{2+}$ overload induced by IP3R activity has been described to occur prior to apoptosome formation, and seems to be a crucial step for global caspases activation, which can in turn lead to IP3R cleavage and dysregulation (43). Additionally, under high $Ca^{2+}$ concentration conditions, calpains are also involved in the N-terminal degradation of the IP3R, leading to constitutive activation and further $Ca^{2+}$ depletion of the ER (44) (Fig. 9). The degradation of the IP3R N-terminal region (which carries the IP3-binding site) would explain why in our study the knockdown of PLC-encoding genes or the chemical inhibition of PLC did not lead to a significant beneficial effect upon muscle degeneration. Indeed, PLC is required to generate IP3. Thus, if, in dystrophic muscles, the $Ca^{2+}$ transient through IP3R were no longer regulated by IP3 release, PLC inactivation would have no effect. However, we cannot rule out the possibility that other PLC homologs, than the six described so far in *C. elegans* (35,45), exist and interact with ITR-1 in the muscle degenerative process. After all, it remains unclear whether cytochrome *c* plays a direct role in apoptosome formation in *C. elegans*.

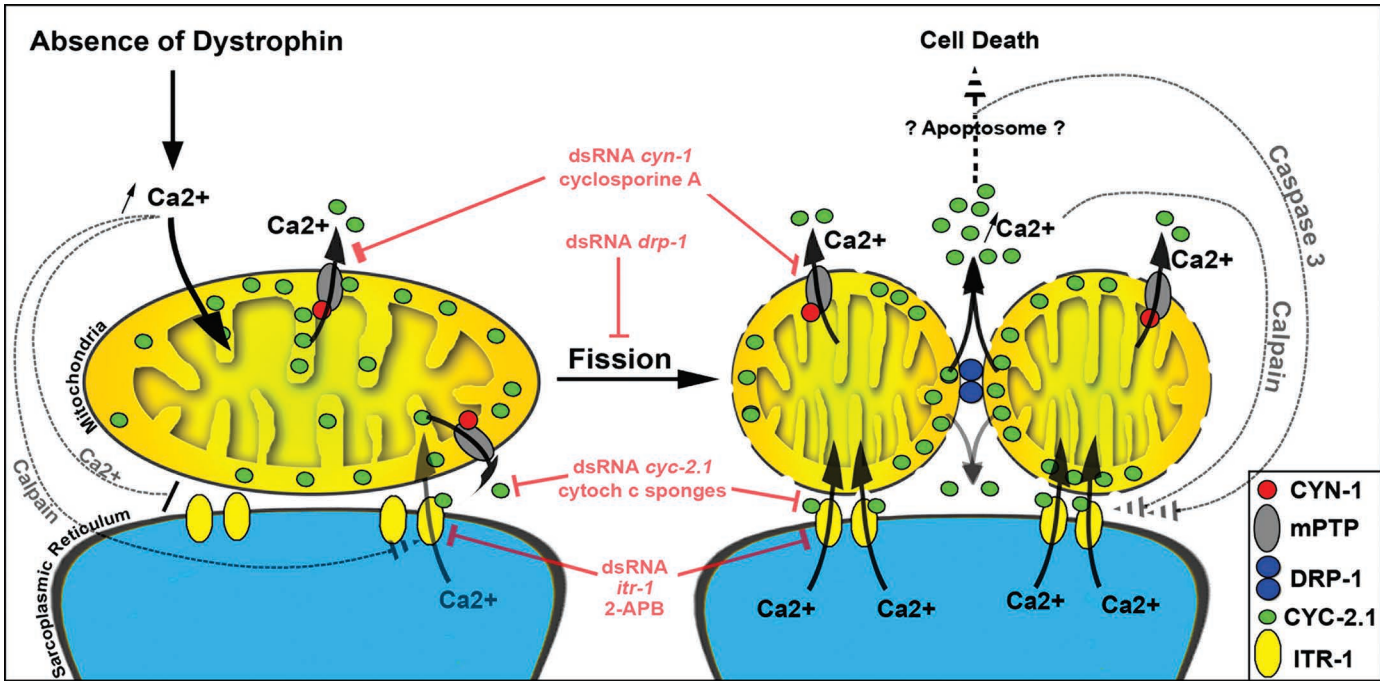


**Figure 9.** Schematic representation of pathways rescuing the dystrophin-deficient muscular degeneration in *C. elegans* in regard to mitochondrial dynamics.

However, our data suggest that this protein may amplify mitochondrial $Ca^{2+}$ overload and subsequently contributes to cell death. More experiments need to be performed to fully understand its role in cell death pathways in *C. elegans*.

Mitochondrial disorders are associated with a large panel of pathologies including muscle diseases (46). Defects in mitochondrial localization and mitochondrial functions were recently reported in the *mdx* mouse model for DMD (47). However, it remains to be established whether and how these defects contribute to the muscle degenerative process and could be targeted in order to reduce the progression of muscle degeneration. Physiologic mitochondrial functions are maintained by the interplay of fusion and fission processes (11). We show that in dystrophic *C. elegans* muscles, mitochondrial fission predominates and that the inactivation of the fission-promoting gene *drp-1* is beneficial toward muscle degeneration. Moreover, increased mitochondrial fission upon muscle degeneration does not seem to be restricted to *C. elegans* since mitochondrial fragmentation is also an early hallmark of muscle degeneration in a zebrafish model for DMD. These observations suggest that mitochondrial morphology alterations could be a universal pattern of dystrophic muscles and an early process in the progression of dystrophin-dependent muscle degeneration. Thus, targeting mitochondrial dynamics could provide therapeutic strategies for muscle diseases.

## CONCLUSION

Our results suggest that CsA treatment may be useful against DMD. Indeed, even if a recent clinical trial shows no direct evidence of its interest for patients, except for its anti-inflammatory effect in regard to gene and cell therapy, a beneficial effect on muscle degeneration at low dose has potentially been missed. It seems that its effect on mPT through cyclophilin D inhibition is key to the muscle protection observed in the *C. elegans* DMD model and requires the application of low doses of CsA. Our study also revealed that mitochondrial dynamics plays an early and crucial role in muscle degeneration. Targeting mitochondrial permeability and dynamics should be explored further in order to establish whether their modulation could delay the progression of the disease in humans. In this regard, the use of Debio025 or other specific mPTP inhibitor might be more relevant than CsA in new clinical trials.

Additionally, this study suggests for the first time, to our knowledge, that (i) mPT may exist in *C. elegans*, and (ii) cytochrome *c* can be implied in muscle cell death in the nematode, at least through its interaction with the calcium channel IP3R, and that their interplay seems to play a role in mitochondrial dynamics.

## MATERIALS AND METHODS

### Strains and culture conditions

*C. elegans* strains were cultured at 15°C on 55 mm Petri dishes containing nematode growth medium (NGM) agar and a lawn of *Escherichia coli* OP50 unless stated otherwise. The following *C. elegans* strains were used: wild-type N2, LS292 *dys-1(cx18)* I, PD4613 *hlh-1(cc561)* II, LS587 *dys-1(cx18)* I;*hlh-1(cc561)* II, PD4251 *ccIs4251* I;*dpy-20(e1282)* IV, LS541 *dys-1(cx18) ccIs4251* I, LS762 *ccIs4251* I;*hlh-1(cc561)* II and LS761 *dys-1(cx18) ccIs4251* I;*hlh-1(cc561)* II;*dpy-20(e1282)* IV (Supplementary Material, Table S1). The *ccIs4251* transgene contains Pmyo-3::Ngfp-lacZ (nuclear GFP localization) and Pmyo-3::Mtgfp (mitochondrial GFP localization). All strains

were grown at 15°C, which is the permissive temperature for the thermo-sensitive mutation *hlh-1(cc561)* (4). The N2, PD4613 and PD4251 strains were obtained from the *Caenorhabditis* Genetics Center.

### Preparation of chemical compounds and drug-containing plates

All pharmacologic compounds were obtained from Sigma Chemical Co. (St Louis, MO, USA). Methazolamide (Meth) was used as a positive control to reduce muscle degeneration ( 8). Concentrated solutions (10×) of each drug were prepared in DMSO. *C. elegans* tolerates DMSO up to a final concentration of 2% vol/vol. Compounds were added to liquid NGM agar that had been autoclaved and cooled to 55°C, and the media was immediately mixed and dispensed into Petri dishes. Depending on the experiment, a drop of *E. coli* OP50 bacteria, empty plasmid L4440 containing HT115 bacteria or HT115 bacteria expressing dsRNA were added on top of the medium. *C. elegans* is permeable to aqueous and organic molecules, and it is admitted that drugs penetrate the worms both by diffusion through the cuticle and ingestion (8). Drugs used in this study were CsA, Meth, 2-APB, U-73122 hydrate.

### Preparation of RNAi plates and generation of dsRNA-expressing bacteria

RNAi experiments were performed on NGM plates supplemented with 100 μg/ml ampicillin, 12.5 μg/ml tetracycline and 2 mM IPTG (NGM-ATI). For each bacteria clone carrying an RNAi plasmid, one colony was cultured overnight at 37°C in 2 ml of LB medium supplemented with 100 μg/ml ampicilin and 12.5 μg/ml tetracycline (LBAT). The day after, 0.01 volume of this preculture was added in 1 volume of LBAT and incubated at 37°C. When the culture had reached 0.45–0.5 DO, 2 mM IPTG was added. At 0.7 DO, 100 to 200 μl of the bacteria culture was seeded on NGM-ATI plates. Plates were allowed to dry at room temperature for at least 3 days before experiments. HT115 bacteria strains producing dsRNA for *cyn-2*, *cyn-3*, *cyn-4*, *cyn-6*, *cyn-8*, *cyn-9*, *cyn-11*, *cyn-12*, *itr-1*, *plc-1*, *plc-2*, *plc-3*, *plc-4*, *pll-1*, *egl-8*, *cyc-1*, *cyc-2.1*, *cyc-2.2*, *drp-1*, *cah-4* and *pos-1* were obtained from the *C. elegans* RNAi library (48). Clones for *cyn-1*, *cyn-5*, *cyn-7*, *cyn-10*, *cyn-13*, *cyn-14*, *cyn-15* and *cyn-16* were constructed for the study. Constructs were obtained by amplification of ∼400–600 pb of genomic DNA of either gene and cloned into the RNAi feeding vector L4440 (for primers, see Supplementary Material, Fig. S9). Note that *pos-1* knockdown is used as an RNAi efficiency control in every experiments, which resulted in nearly 100% embryonic lethality.

### Drug and/or RNAi assays

Three gravid adults of the N2, PD4251, LS292, LS541 or LS762 strains and five gravid adults of the LS587 or LS761 strains were put on plates for one night and removed, so as progeny was exposed to drug and/or dsRNA from hatching to fixation. All worms were fixed and observed at day 8 of culture, unless stated otherwise. Before collecting each population, the plates were observed to ensure that the bacteria layer has not been depleted before the end of the assay. As RNAi efficiency control, *pos-1* RNAi knockdown performed in parallel resulted in nearly 100% embryonic lethality. As RNAi-negative control, plates seeded with empty plasmid L4440 containing bacteria were used. All experiments were performed in duplicate and were repeated at least three times.

### Scoring of muscle degeneration

The 95 body-wall muscles of *C. elegans* are organized into four quadrants (ventral right and left, dorsal right and left) each of which consists of 23 or 24 diamond-shaped muscle cells, arranged in two staggered rows (Supplementary Material, Fig. S1). Unless stated otherwise, muscle observation was performed on worms after 8 days of culture at 15°C. All worms were collected and fixed for 1 h in 1 ml of PBS supplemented with 30 μl of 37% formaldehyde. Each sample was stained by rhodamine-coupled phalloidin, a marker of filamentous actin. Staining was performed according to Waterston *et al.* (49). Slides were observed on a Zeiss Axioplan microscope. A body-wall muscle cell is considered degenerating when its actin fibers are fragmented or destroyed (Supplementary Material, Fig. S1B) (4). Only the two most visible muscle quadrants of each animal were scored. A minimum of 20 worms per conditions were examined per experiments. Experiments were repeated three to five times. Numbers were compared by a Student's *t*-test.

### Locomotion and growth rate

To estimate the locomotion rate of nematodes, worms cultured for 8 days at 15°C were scored for the number of body bends generated during an interval of 1 min on NGM plates without bacteria. A body bend was defined as one complete sinusoidal movement from maximum to minimum amplitude and back again. The growth rate refers to the time from F0 eggs to the first F1 eggs (generation time). A minimum of 20 worms were examined. Numbers were compared by a Student's *t*-test.

### *cyc-2.1*::GFP construct and localization

Approximately 1 kb upstream of the ATG start codon of *cyc-2.1* was amplified by PCR (forward primer: AATTGTCGACCCACTTCGCCTAAGTTGCGG; reverse primer: AATTACCGGTGTTGAACCCTTAAAATACAG). This fragment containing the putative endogenous promoter of the *cyc-2.1* gene was cloned upstream of the GFP-encoding sequence in pPD95.75 (kindly provided by A. Fire, Stanford University School of Medicine), resulting in plasmid pJG03. Wild-type N2 hermaphrodite young adults were injected with 25 ng/μl pCFJ68 (P*unc-122*::GFP) as selection marker (Addgene), and 10 ng/μl P*cyc-2.1*::GFP containing plasmid. Plasmid microinjection was performed as described (50). Individual F1 worms expressing GFP in coelomocytes (due to the expression of the Punc-122::GFP transgene) were isolated. Four independent stable transgenic lines were isolated, as defined by F1 giving transgenic progeny. Transgenic worms (50, all stages) were observed using a fluorescence microscopy on a Zeiss LSM 510 Meta fluorescence confocal microscope so as to detect the expression pattern of the P*cyc-2.1*::GFP transgene.

### Confocal imaging and image treatment

All *C. elegans* images presented in this manuscript were recorded using a Zeiss LSM 510 Meta fluorescence confocal microscope at room temperature, and the files were processed and converted under ImageJ environment.

### Mitochondrial morphology analysis

For mitochondrial analysis, *C. elegans* strains were grown at 15°C for 6, 7, 8 and 9 days in the presence or absence of drugs and/or specific dsRNA-expressing bacteria. Worms were collected with PBS and fixed with formaldehyde (0.37% final), 15 min at room temperature under agitation. Samples were then washed three times with PBS to remove formaldehyde, mounted on slides with DAKO mounting medium and observed under a Zeiss LSM 510 Meta fluorescence confocal microscope the same day.

To score mitochondria morphology, approximately 16 body-wall muscle cells per animal were observed. These 16 body-wall muscle cells belonged to 1 quadrant (Supplementary Material, Fig. S1), excluding the first 4 anterior cells in the head and the last 4 posterior cells in the tail. These cells were excluded, as they are less subject to degeneration and difficult to analyze due to their small size and their heterogeneous mitochondrial pattern. Individual muscle cell mitochondrial pattern was categorized as (i) tubular, (ii) fragmented, (iii) intermediate or (iiii) absent. Interconnected mitochondria profile, as described by Tan *et al.* (12), was also observed in some muscle cells of the LS762 strain. However, these cells were classified as tubular. The mitochondrial pattern of a given muscle cell was stated as 'tubular' if almost all mitochondria had a length/width ratio of $>2$, 'fragmented' if most of the mitochondria had a spherical pattern (length/width ratio of $\sim 1$), 'intermediate' if one can clearly observe a mix of tubular and fragmented pattern. All experiments were performed in duplicate and were repeated at least three times.

### IP3R sequence comparison

IP3R sequences were obtained from the NCBI website. *Homo sapiens* type 1 isoform 1, NP_001093422.2; *Mus musculus* type 1, NP_034715.3; *Rattus norvegicus* type 1, NP_001007236.1; *Danio rerio* type 1, XP_696007.5; *Drosophila melanogaster* isoform B, AAN13240.1 and *C. elegans*, NP_001023173.1. Cytochrome *c*-binding domain was identified in the different sequences by alignment studies using the amino acids 2621–2636 of the type I IP3R rat sequence published by Boehning *et al.* (31). Alignments were performed with MUSCLE, Multiple Sequence Comparison by Log-Expectation. Alignment presented in Figure 6 was designed manually under Photoshop environment based on MUSCLE alignment.

### Cytochrome *c* sponge generation and expression in *C. elegans*

To amplify the cytochrome *c* binding sequence encoded by the *itr-1* gene, a PCR fragment encompassing the full *itr-1* C-terminal sequence (starting from the end of the last transmembrane domain) was amplified using *C. elegans* cDNA material (primers available in Supplementary Material, Fig. S9) (this fragment encodes ITR-1 amino acids sequence 2703–2846 and is named Sp-cyc). An HA-tag sequence was introduced in the 3′ primer for the construct Sp-cyc-HA to allow *in situ* validation of the peptide expression in the nematode. In addition, forward and reverse primers contained an *Xba*I and *Nco*I site, respectively. PCR products were introduced in the *Xba*I/*Nco*I sites of the pKG123 plasmid, downstream of a muscle-specific promoter (P*myo-3*) and upstream of the *unc*-54 3′UTR. Resulting plasmids were named pKG160 and pKG159, respectively. Young adult hermaphrodites of the N2 strain were injected with 25 ng/µl pKG160 (*Pmyo-3*::Sp-cyc::HA-tag::*unc-54* 3′UTR) or pKG159 (P*myo-3*::Sp-cyc::*unc-54* 3′UTR) and with (i) 2.5 ng/µl pCFJ90 (P*myo-2*::mCherry) as selection marker (Addgene) for the construct with HA tag, or (ii) with 2.5 ng/µl pCFJ90 (P*myo-2*::mCherry) and 5 ng/µl pCFJ104 (P*myo-3*::mCherry) (Addgene) as selection markers for the construct without an HA tag. Plasmid microinjection was performed as described (50). Individual wild-type F1 expressing mCherry in pharyngeal muscles were isolated and two different lines retained for each construct that were positive for the injection marker in the F2 generation. Transgenics lines were then crossed with the LS761 line to test the effect of tagged or not tagged sponges against muscle degeneration. Expression of the Sp-cyc-HA construct was assessed in N2, checking the presence of a mosaic HA signal in the muscle tissue. Worms were analyzed by immuno-chemistry on whole-mount preparations as described by Benian *et al.* (51). Secondary Alexa 555 goat anti-mouse antibody (Invitrogen) was used to reveal the primary mouse anti-HA antibody (Santa Cruz). Imaging was carried out as stated above.

### Yeast two-hybrid experiments

To carry out this yeast two-hybrid assays, bait and prey vectors from Clontech (Palo Alto, CA, USA) were used. The pAS2-1 bait plasmid contains the Gal4 DNA binding domain (Gal4-BD) upstream of a polylinker. The pACT-2 prey plasmid contains the Gal4 activation domain (Gal4-AD) upstream of a polylinker.

The coding sequences of CYC-2.1 (amino acids 1–111) and ITR-1 C-ter (amino acids 2703–2846, named Sp-cyc) were amplified by PCR using *C. elegans* cDNA with the use of appropriate primers integrating *Nco*I and *Xma*I restriction sites, respectively, at 5′ and 3′ ends of each PCR product (Supplementary Material, Fig. S9). For the Sp-cyc-HA construct, the same ITR-1 C-ter (amino acids 2703–2846) coding sequence as for SP-cyc was amplified by PCR; the HA coding sequence was integrated to the PCR product through the 3′ primer (Supplementary Material, Fig. S9). All PCR products were digested by *Nco*I/*Xma*I and cloned into the *Nco*I/*Xma*I sites of the pACT2 as well as the pAS2-1 plasmids. The resulting bait plasmids were named pKG162 (Sp-cyc sequence in pAS2-1), pKG164 (Sp-cyc-HA in pAS2-1), pKG166 (*cyc-2.1* in pAS2-1); the resulting prey plasmids were named pKG161 (Sp-cyc sequence in pACT2), pKG163 (Sp-cyc-HA in pACT2), pKG165 (*cyc-2.1* in pACT2). Bait plasmids were transformed into the yeast strain CG1945 and prey plasmids into the yeast strain Y187 using the LiAc transformation procedure (Clontech, Yeast protocols Handbook, PT 3024-1). Interactions

between Sp-cyc, Sp-cyc::HA and CYC-2.1 were assayed as described (52) after mating of transformed CG1945 yeast cells with the transformed Y187 yeast cells. Ten microliters of mating cultures were deposed on minimal medium lacking Leu and Trp (growth control) or minimal medium lacking leucine (Leu), tryptophan (Trp) and histidine (His) on which yeast can only grow if the prey and bait proteins interact, and incubated for 3 days at 30°C. The 3-AT competitive inhibitor (3-amino-1,2,4-triazol) was added at a final concentration of 30 mM, when the Sp-cyc::HA construct was used as bait.

### Phylogenetic analyses

A Blastp search was performed on *C. elegans* genome (taxid: 6239) with six *M. musculus* cyclophilin sequences obtained from the NCBI website as query sequence: cyclophilin A (NP_032933.1), cyclophilin C (AAA37511.1), cyclophilin D (AAH19778.1), cyclophilin E (AAH45154.1), cyclophilin F (AAH04041.1), cyclophilin G (AAI50695.1). The *C. elegans* sequences selected are CYN-1 (CAB07303.1), CYN-2 (NP_499828.1), CYN-3 (CAA21762.1), CYN-4 (CAA85 417.1), CYN-5 (CAB07192.1), CYN-6 (CCD61884.1), CYN-7 (CAA21760.1), CYN-8 (CCD64413.1), CYN-9 (CAA88291.1), CYN-10 (CCD61542.1), CYN-11 (CAA91297.1), CYN-12 (CCD66606.1), CYN-13 (CBK19486.1), CYN-14 (CAB0 3088.2), CYN-15 (CAB60429.1), CYN-16 (CAA19454.2). A maximum likelihood tree was constructed using SEAVIEW version 4.0, based on MUSCLE alignment (MUltiple Sequence Comparison by Log-Expectation). The *C. elegans* carbonic anhydrase 4 (CAH-4) sequence (CAA92190.2) was used as an outgroup. The bootstrap was performed with 500 replicates.

### Zebrafish strains, injection, sorting and imaging

The $dmd^{pc2+/-}$ zebrafish line was described in Berger *et al*. (25). Zebrafish were bred and maintained by standard protocols approved by MAS/2009/05. All experiments were approved also by the University of Sydney Animal Ethics Committee. In aiming to express GFP in zebrafish muscle mitochondria, pSCAC-69 plasmid (courtesy of Dr Seok-Yong Choi), which carries GFP sequence with a mitochondrial targeting signal, was digested by *Xho*I/*Hin*dIII to remove the pEF1A promoter. Polymerase I large Klenow fragment was then used to generate blunt end. Muscle-specific alpha-actin promoter was cut from P5EA-acta1 plasmid (courtesy of Thomas Hall) using *Ava*I/*Eco*RI, made blunt and cloned upstream of the GFP sequence, final plasmid was named JG013. Thirty picograms of JG013 plasmid were injected into one-cell-stage embryos obtained by incrossing $PC2^{+/-}$ animals. GFP-positive embryos were sorted using a fluorescent stereo-microscope at 1 d.p.f. Homozygous DMD $dmd^{pc2+/+}$ larvae start to die from 9 d.p.f. and can usually not survive more than 30 d.p.f. Homozygous $dmd^{pc2+/+}$ embryos and larvae can, therefore, only be obtained by crossing heterozygous $dmd^{pc2+/-}$ adults. Homozygous $dmd^{pc2+/+}$ embryos were detected, at 3 d.p.f., by birefringence using polarized light and two circular polarized filters. $dmd^{pc2-/-}$ and $dmd^{pc2+/-}$ control siblings and $dmd^{pc2+/+}$ embryos and larvae were mounted in 1% low-melting agarose supplemented with 0.02% tricaine and scanned using an LSM710 confocal microscope.

## AUTHORS' CONTRIBUTIONS

J.G. designed research; J.G and N.B. performed research; M.-C.M and L.S. generated LS587, LS541, LS762 and LS761 *C. elegans* strains; J.B. and P.D.C. generated $dmd^{pc2}$ zebrafish line; L.W. and T.S.B. were involved in the review process; J.G. analyzed data and J.G. and K.G. wrote the manuscript.

## SUPPLEMENTARY MATERIAL

Supplementary Material is available at *HMG* online.

## ACKNOWLEDGEMENTS

The authors wish to thank the *Caenorhabditis* Genetics Center (CGC) for providing nematode strains, Caroline Borrel for the management of the Geneservice RNAi Library, Adam Svahn for helpful comments on this manuscript and Stefan Jünemann for sharing unpublished results on ITR-1. We thank Dr Andrew Fire for the gift of the pPD95.75 plasmid, Dr Thomas Hall for the p5EA-acta1 plasmid and Dr Seok-Yong Choi for the pSCAC-69 plasmid.

*Conflict of Interest statement.* None declared.

## FUNDING

This work was supported by the Association Française contre les Myopathies (AFM, contract AFM_tireur, hors AO-2006) and by the French Agence Nationale de la Recherche (ANR, Projet DUCHENNE_ELEGANS—ANR-07-MRAR-005). J.G. was also supported by the National Health and Medical Research Council of Australia (grant number APP1024863). P.D.C. and J.B. were supported by the National Health and Medical Research Council of Australia (grant number 1024482) and the Muscular Dystrophy Association USA (grant number 201098).

## REFERENCES

1. Koenig, M., Hoffman, E.P., Bertelson, C.J., Monaco, A.P., Feener, C. and Kunkel, L.M. (1987) Complete cloning of the Duchenne muscular dystrophy (DMD) cDNA and preliminary genomic organization of the DMD gene in normal and affected individuals. *Cell*, **50**, 509–517.
2. Rando, T.A. (2001) The dystrophin-glycoprotein complex, cellular signaling, and the regulation of cell survival in the muscular dystrophies. *Muscle Nerve*, **24**, 1575–1594.
3. Manzur, A.Y., Kuntzer, T., Pike, M. and Swan, A. (2008) Glucocorticoid corticosteroids for Duchenne muscular dystrophy. *Cochrane Database Syst. Rev.*, CD003725.
4. Gieseler, K., Grisoni, K. and Segalat, L. (2000) Genetic suppression of phenotypes arising from mutations in dystrophin-related genes in *Caenorhabditis elegans*. *Curr. Biol.*, **10**, 1092–1097.
5. Giacomotto, J. and Segalat, L. (2010) High-throughput screening and small animal models, where are we? *Br. J. Pharmacol.*, **160**, 204–216.
6. Giacomotto, J., Segalat, L., Carre-Pierrat, M. and Gieseler, K. (2011) *Caenorhabditis elegans* as a chemical screening tool for the study of neuromuscular disorders. Manual and semi-automated methods. *Methods*, **56**, 103–113.
7. Carre-Pierrat, M., Lafoux, A., Tanniou, G., Chambonnier, L., Divet, A., Fougerousse, F., Huchet-Cadiou, C. and Segalat, L. (2011) Pre-clinical study of 21 approved drugs in the mdx mouse. *Neuromuscul. Disord.*, **21**, 313–327.
8. Giacomotto, J., Pertl, C., Borrel, C., Walter, M.C., Bulst, S., Johnsen, B., Baillie, D.L., Lochmuller, H., Thirion, C. and Segalat, L. (2009) Evaluation

of the therapeutic potential of carbonic anhydrase inhibitors in two animal models of dystrophin deficient muscular dystrophy. *Hum. Mol. Genet.*, **18**, 4089–4101.
9. Mariol, M.C. and Segalat, L. (2001) Muscular degeneration in the absence of dystrophin is a calcium-dependent process. *Curr. Biol.*, **11**, 1691–1694.
10. Mariol, M.C., Martin, E., Chambonnier, L. and Segalat, L. (2007) Dystrophin-dependent muscle degeneration requires a fully functional contractile machinery to occur in *C. elegans*. *Neuromuscul. Disord.*, **17**, 56–60.
11. Chan, D.C. (2012) Fusion and fission: interlinked processes critical for mitochondrial health. *Annu. Rev. Genet.*, **46**, 265–287.
12. Tan, F.J., Husain, M., Manlandro, C.M., Koppenol, M., Fire, A.Z. and Hill, R.B. (2008) CED-9 and mitochondrial homeostasis in *C. elegans* muscle. *J. Cell Sci.*, **121**, 3373–3382.
13. Detmer, S.A. and Chan, D.C. (2007) Functions and dysfunctions of mitochondrial dynamics. *Nat. Rev. Mol. Cell Biol.*, **8**, 870–879.
14. Green, D.R. and Kroemer, G. (2004) The pathophysiology of mitochondrial cell death. *Science*, **305**, 626–629.
15. Wang, X. (2001) The expanding role of mitochondria in apoptosis. *Genes Dev.*, **15**, 2922–2933.
16. Baines, C.P., Kaiser, R.A., Purcell, N.H., Blair, N.S., Osinska, H., Hambleton, M.A., Brunskill, E.W., Sayen, M.R., Gottlieb, R.A., Dorn, G.W. *et al.* (2005) Loss of cyclophilin D reveals a critical role for mitochondrial permeability transition in cell death. *Nature*, **434**, 658–662.
17. Tiepolo, T., Angelin, A., Palma, E., Sabatelli, P., Merlini, L., Nicolosi, L., Finetti, F., Braghetta, P., Vuagniaux, G., Dumont, J.M. *et al.* (2009) The cyclophilin inhibitor Debio 025 normalizes mitochondrial function, muscle apoptosis and ultrastructural defects in Col6a1 −/− myopathic mice. *Br. J. Pharmacol.*, **157**, 1045–1052.
18. Matsuda, S. and Koyasu, S. (2000) Mechanisms of action of cyclosporine. *Immunopharmacology*, **47**, 119–125.
19. De Luca, A., Nico, B., Liantonio, A., Didonna, M.P., Fraysse, B., Pierno, S., Burdi, R., Mangieri, D., Rolland, J.F., Camerino, C. *et al.* (2005) A multidisciplinary evaluation of the effectiveness of cyclosporine a in dystrophic mdx mice. *Am. J. Pathol.*, **166**, 477–489.
20. Broekemeier, K.M., Dempsey, M.E. and Pfeiffer, D.R. (1989) Cyclosporin A is a potent inhibitor of the inner membrane permeability transition in liver mitochondria. *J. Biol. Chem.*, **264**, 7826–7830.
21. Azzolin, L., von Stockum, S., Basso, E., Petronilli, V., Forte, M.A. and Bernardi, P. (2010) The mitochondrial permeability transition from yeast to mammals. *FEBS Lett.*, **584**, 2504–2509.
22. Claros, M.G. and Vincens, P. (1996) Computational method to predict mitochondrially imported proteins and their targeting sequences. *Eur. J. Biochem.*, **241**, 779–786.
23. Fire, A., Xu, S., Montgomery, M.K., Kostas, S.A., Driver, S.E. and Mello, C.C. (1998) Potent and specific genetic interference by double-stranded RNA in *Caenorhabditis elegans*. *Nature*, **391**, 806–811.
24. Kamp, F., Exner, N., Lutz, A.K., Wender, N., Hegermann, J., Brunner, B., Nuscher, B., Bartels, T., Giese, A., Beyer, K. *et al.* (2010) Inhibition of mitochondrial fusion by alpha-synuclein is rescued by PINK1, Parkin and DJ-1. *EMBO J.*, **29**, 3571–3589.
25. Berger, J., Berger, S., Jacoby, A.S., Wilton, S.D. and Currie, P.D. (2011) Evaluation of exon-skipping strategies for Duchenne muscular dystrophy utilizing dystrophin-deficient zebrafish. *J. Cell. Mol. Med.*, **15**, 2643–2651.
26. Kim, M.J., Kang, K.H., Kim, C.H. and Choi, S.Y. (2008) Real-time imaging of mitochondria in transgenic zebrafish expressing mitochondrially targeted GFP. *Biotechniques*, **45**, 331–334.
27. Zamzami, N. and Kroemer, G. (2001) The mitochondrion in apoptosis: how Pandora's box opens. *Nat. Rev. Mol. Cell Biol.*, **2**, 67–71.
28. Vincelli, A.J., Pottinger, D.S., Zhong, F., Hanske, J., Rolland, S.G., Conradt, B. and Pletneva, E.V. (2013) Recombinant expression, biophysical characterization, and cardiolipin-induced changes of two *Caenorhabditis elegans* cytochrome *c* proteins. *Biochemistry*, **52**, 653–666.
29. Abdelwahid, E., Rolland, S., Teng, X., Conradt, B., Hardwick, J.M. and White, K. (2011) Mitochondrial involvement in cell death of non-mammalian eukaryotes. *Biochim. Biophys. Acta*, **1813**, 597–607.
30. Boehning, D., Patterson, R.L., Sedaghat, L., Glebova, N.O., Kurosaki, T. and Snyder, S.H. (2003) Cytochrome *c* binds to inositol (1,4,5) trisphosphate receptors, amplifying calcium-dependent apoptosis. *Nat. Cell Biol.*, **5**, 1051–1061.
31. Boehning, D., van Rossum, D.B., Patterson, R.L. and Snyder, S.H. (2005) A peptide inhibitor of cytochrome *c*/inositol 1,4,5-trisphosphate receptor binding blocks intrinsic and extrinsic cell death pathways. *Proc. Natl Acad. Sci. USA*, **102**, 1466–1471.
32. Galvan, D.L. and Mignery, G.A. (2002) Carboxyl-terminal sequences critical for inositol 1,4,5-trisphosphate receptor subunit assembly. *J. Biol. Chem.*, **277**, 48248–48260.
33. Walker, D.S., Gower, N.J., Ly, S., Bradley, G.L. and Baylis, H.A. (2002) Regulated disruption of inositol 1,4,5-trisphosphate signaling in *Caenorhabditis elegans* reveals new functions in feeding and embryogenesis. *Mol. Biol. Cell.*, **13**, 1329–1337.
34. Yin, X., Gower, N.J., Baylis, H.A. and Strange, K. (2004) Inositol 1,4,5-trisphosphate signaling regulates rhythmic contractile activity of myoepithelial sheath cells in *Caenorhabditis elegans*. *Mol. Biol. Cell.*, **15**, 3938–3949.
35. Gower, N.J., Walker, D.S. and Baylis, H.A. (2005) Inositol 1,4,5-trisphosphate signaling regulates mating behavior in *Caenorhabditis elegans* males. *Mol. Biol. Cell*, **16**, 3978–3986.
36. Kirschner, J., Schessl, J., Schara, U., Reitter, B., Stettner, G.M., Hobbiebrunken, E., Wilichowski, E., Bernert, G., Weiss, S., Stehling, F. *et al.* (2010) Treatment of Duchenne muscular dystrophy with ciclosporin A: a randomised, double-blind, placebo-controlled multicentre trial. *Lancet Neurol.*, **9**, 1053–1059.
37. Stupka, N., Gregorevic, P., Plant, D.R. and Lynch, G.S. (2004) The calcineurin signal transduction pathway is essential for successful muscle regeneration in mdx dystrophic mice. *Acta. Neuropathol.*, **107**, 299–310.
38. Reagan-Shaw, S., Nihal, M. and Ahmad, N. (2008) Dose translation from animal to human studies revisited. *FASEB J.*, **22**, 659–661.
39. Reutenauer, J., Dorchies, O.M., Patthey-Vuadens, O., Vuagniaux, G. and Ruegg, U.T. (2008) Investigation of Debio 025, a cyclophilin inhibitor, in the dystrophic mdx mouse, a model for Duchenne muscular dystrophy. *Br. J. Pharmacol.*, **155**, 574–584.
40. Millay, D.P., Sargent, M.A., Osinska, H., Baines, C.P., Barton, E.R., Vuagniaux, G., Sweeney, H.L., Robbins, J. and Molkentin, J.D. (2008) Genetic and pharmacologic inhibition of mitochondrial-dependent necrosis attenuates muscular dystrophy. *Nat. Med.*, **14**, 442–447.
41. Palma, E., Tiepolo, T., Angelin, A., Sabatelli, P., Maraldi, N.M., Basso, E., Forte, M.A., Bernardi, P. and Bonaldo, P. (2009) Genetic ablation of cyclophilin D rescues mitochondrial defects and prevents muscle apoptosis in collagen VI myopathic mice. *Hum. Mol. Genet.*, **18**, 2024–2031.
42. Rizzuto, R., Brini, M., Murgia, M. and Pozzan, T. (1993) Microdomains with high Ca2+ close to IP3-sensitive channels that are sensed by neighboring mitochondria. *Science*, **262**, 744–747.
43. Patterson, R.L., Boehning, D. and Snyder, S.H. (2004) Inositol 1,4,5-trisphosphate receptors as signal integrators. *Annu. Rev. Biochem.*, **73**, 437–465.
44. Wojcikiewicz, R.J. and Oberdorf, J.A. (1996) Degradation of inositol 1,4,5-trisphosphate receptors during cell stimulation is a specific process mediated by cysteine protease activity. *J. Biol. Chem.*, **271**, 16652–16655.
45. Vazquez-Manrique, R.P., Nagy, A.I., Legg, J.C., Bales, O.A., Ly, S. and Baylis, H.A. (2008) Phospholipase C-epsilon regulates epidermal morphogenesis in *Caenorhabditis elegans*. *PLoS Genet.*, **4**, e1000043.
46. Vafai, S.B. and Mootha, V.K. (2012) Mitochondrial disorders as windows into an ancient organelle. *Nature*, **491**, 374–383.
47. Percival, J.M., Siegel, M.P., Knowels, G. and Marcinek, D.J. (2013) Defects in mitochondrial localization and ATP synthesis in the mdx mouse model of Duchenne muscular dystrophy are not alleviated by PDE5 inhibition. *Hum. Mol. Genet.*, **22**, 153–167.
48. Kamath, R.S., Fraser, A.G., Dong, Y., Poulin, G., Durbin, R., Gotta, M., Kanapin, A., Le Bot, N., Moreno, S., Sohrmann, M. *et al.* (2003) Systematic functional analysis of the *Caenorhabditis elegans* genome using RNAi. *Nature*, **421**, 231–237.
49. Waterston, R.H., Hirsh, D. and Lane, T.R. (1984) Dominant mutations affecting muscle structure in *Caenorhabditis elegans* that map near the actin gene cluster. *J. Mol. Biol.*, **180**, 473–496.
50. Mello, C. and Fire, A. (1995) DNA transformation. *Methods Cell Biol.*, **48**, 451–482.
51. Benian, G.M., Tinley, T.L., Tang, X. and Borodovsky, M. (1996) The *Caenorhabditis elegans* gene unc-89, required for muscle M-line assembly, encodes a giant modular protein composed of Ig and signal transduction domains. *J. Cell Biol.*, **132**, 835–848.
52. Grisoni, K., Gieseler, K., Mariol, M.C., Martin, E., Carre-Pierrat, M., Moulder, G., Barstead, R. and Segalat, L. (2003) The stn-1 syntrophin gene of C.elegans is functionally related to dystrophin and dystrobrevin. *J. Mol. Biol.*, **332**, 1037–1046.